

Spatial Diversity in Radars - Models and Detection Performance

Eran Fishler[†], Alex Haimovich[†], Rick Blum[‡], Len Cimini^o, Dmitry Chizhik^{*}, Reinaldo
Valenzuela^{*}

The work of Eran Fishler was supported by the New Jersey Center for Wireless Telecommunications. The work of Alexander Haimovich was supported in part by the Air Force Office of Scientific Research under Grant No. F49620-03-1-0161. The work of Rick Blum is based on research supported by the Air Force Research Laboratory under Grant No. F49620-03-1-0214.

[†] New Jersey Institute of Technology, Newark, NJ 07102, e-mail: {eran.fishler, haimovic}@njit.edu

[‡] Lehigh University, Bethlehem, PA 18015-3084, e-mail: rblum@eecs.lehigh.edu

^o University of Delaware, Newark, DE 19716, e-mail: cimini@ece.udel.edu

^{*} Bell Labs - Lucent Technologies, e-mail: chizhik,rav@lucent.com

Abstract

Inspired by recent advances in multiple-input multiple-output (MIMO) communications, this proposal introduces the statistical MIMO radar concept. To our knowledge, this is the first time that the statistical MIMO is being proposed for radar. The fundamental difference between statistical MIMO and other radar array systems is that the latter seek to maximize the coherent processing gain, while statistical MIMO radar capitalizes on the diversity of target scattering to improve radar performance. Coherent processing is made possible by highly correlated signals at the receiver array, whereas in statistical MIMO radar, the signals received by the array elements are uncorrelated. Radar targets generally consist of many small elemental scatterers that are fused by the radar waveform and the processing at the receiver, to result in echoes with fluctuating amplitude and phase. It is well known that in conventional radar, slow fluctuations of the target radar cross section (RCS) result in target fades that degrade radar performance. By spacing the antenna elements at the transmitter and at the receiver such that the target angular spread is manifested, the MIMO radar can exploit the spatial diversity of target scatterers opening the way to a variety of new techniques that can improve radar performance. In this paper, we focus on the application of the target spatial diversity to improve detection performance. The optimal detector in the Neyman-Pearson sense is developed and analyzed for the statistical MIMO radar. It is shown that the optimal detector consists of non-coherent processing of the receiver sensors' outputs and that for cases of practical interest, detection performance is superior to that obtained through coherent processing. An optimal detector invariant to the signal and noise levels is also developed and analyzed. In this case as well, statistical MIMO radar provides great improvements over other types of array radars.

I. INTRODUCTION

Radar theory has been a vibrant scientific field for the last fifty years or so [1], [2], [3]. Radar theory deals with many different and diverse problems. However, the two most important problems are the detection and range estimation problems. The importance of these two problems is not limited to radars, and other engineering disciplines like sonar and communication deal with very similar problems [4]. Over the years, radar systems have developed considerably. These developments can be attributed to the increase in computation power and advances in hardware design. While early radar systems utilized a directional antenna, today's array radar systems can synthesize beams and simultaneously scan the whole space [5].

In array radars, the system is composed of many closely spaced omni-directional antennas that either transmit or receive signals. Nonetheless, in some radar systems, only one antenna transmits energy. Such systems are known as active radars [6], [7]. In active radar systems, the transmitting antenna transmits a known waveform. This waveform is reflected back from the target toward the receiving array. The radar system's tasks are to detect the existence of the target and to estimate its unknown parameters, e.g., range, speed, and direction.

In active array applied to radar systems, solutions for the detection and parameter estimation problems are well documented in the literature (see, the survey in [8]). These solutions can be divided into two groups. The first group of solutions is based on high resolution techniques, e.g., MUSIC or maximum likelihood (ML) [8]. In the second group of solutions, the array of sensors is used to steer a beam toward a certain direction in space, in a manner similar to a conventional radar with a directional antenna [5]. The advantages of array radars are well known (see, for example [9], [5], [8], [10], [11]). The lack of any

mechanical elements in the system and the ability to steer multiple beams at once are two examples of such advantages.

Systems with more than one transmitting element have been proposed and built as well [9]. In these systems, an array of transmitting elements is used. In the conventional approach, an array of closely spaced transmitting elements is used to cohere a beam toward a certain direction in space, a process called *beamforming* [5]. The main advantage of these systems is the lack of any mechanical elements, which reduces the system's complexity and improves its performance.

Recently a new and interesting concept in array radar has been introduced by the synthetic impulse and aperture radar (SIAR) [12], [13], [14]. In SIAR systems, the elements of the transmitting array emit orthogonal waveforms. Through synthetic pulse formation, SIAR achieves the advantages of wideband radar (improved range resolution) while individual antennas transmit narrowband waveforms. Unlike conventional beamformers, SIAR features isotropic radiation (an advantage in terms of the probability of intercept of the radar waveform by a third party). But, like beamformers, SIAR exploits the full correlation of signals transmitted and received at the array elements. Radars utilizing multiple transmitters and orthogonal waveforms have also been proposed in [15], [16], where they have been referred to as MIMO radars.

The performance of radar systems is limited by target scintillations [17]. Targets are complex bodies composed of many scatterers. The range to, and the orientation of, the target determines the amount of energy reflected from these scatterers, and small changes in range or orientation can result in a large increase or decrease in the amount of energy reflected from the target [17], [4]. Both experimental measurements and theoretical results demonstrate that scintillations of 10 dB or more in the reflected energy can occur by changing the target aspect by as little as one milliradian [2]. These scintillations are responsible for signal fading, which can cause a large degradation in the system's performance.

Most, if not all, radar processing ignores target scintillations and considers target scintillations as an unavoidable loss. Target radar cross section (RCS) fading can reduce the received signal energy to a level that does not allow reliable detection. One way to mitigate the effect of target fading is to maximize the received energy from the target. This in turn implies that one should maximize the system's coherent processing gain. Since processing gain can be realized with closely spaced antennas, most systems use an array of closely spaced antennas.

Motivated by recent developments in communication theory [18], we question the conventional wisdom of maximizing the coherent processing gain. In this paper, we demonstrate that there are alternative optimization criteria that outperform beamforming and leads to a new radar architecture. In particular, we demonstrate that the utility of an array of sensors in which the spacing between the elements of the array is very large, and that orthogonal waveforms should be transmitted from the elements of the transmitting array. The key point in the radar architecture is that sensors both at the transmitter and the

receiver of the radar are separated such that they experience an *angular spread*¹. As will be seen in the sequel, such a system forms a multistatic radar. The advantage of this system is that the average received energy (averaged across all the independent radars) is approximately constant, i.e., it does not fade as in conventional systems. In essence, we will show that spatial diversity gain outweighs the coherent processing gain. We will demonstrate that an additional advantage of such systems is that the sensor outputs are combined non-coherently.

Communication systems that use the same principle for improving their performance are called Multiple Input Multiple Output (MIMO) systems. Since our proposed system is inspired by MIMO communications, and it exploits that statistical properties of the target RCS, we refer to it as *statistical MIMO radar*. The reader should note that the whole notion of statistical MIMO radar is new, and the main purpose of this paper is to introduce this concept and to demonstrate its advantages. For clarity and mathematical tractability we use a simple model which ignores Doppler effects and clutter. More realistic models are left to subsequent work.

The rest of the paper is organized as follows: Section II develops a signal model that generalizes current signal models. This model is then used to classify different array radars and in particular to describe our proposed statistical MIMO radar. Section III analyzes the performance of the proposed radar, while Section IV examines the optimal invariance detector. Section V provides the summary and concluding remarks.

II. SIGNAL MODEL

A. General Theory

The point source assumption dominates the models used in radar theory [2]. For closely spaced sensors and large range between the target and the array, the point source assumption is an excellent approximation. However, as has been noted in the array signal processing community, a more accurate model is the distributed source model [19], [20], [21]. Unlike the common point source model, the distributed source model accounts for the spatial characteristics of the target. In statistical MIMO radar, the spacing between the array elements is large. Due to the target's complex shape and the distance between the array elements, every element observes a different aspect of the target. Therefore, the point source model is not adequate for describing the received signal in statistical MIMO radar, and a more detailed model must be developed.

In what follows we assume that the target is located at some point (x_0, y_0) in space, and it is stationary during the observation time, i.e, Swerling I model [2]. The target has a rectangular shape whose dimensions are $\Delta x \times \Delta y$ meters. In addition, we assume that our system is composed of M transmitters and N receivers. With reference to Figure 1, denote by (tx_k, ty_k) , $k = 1, \dots, M$, the locations (in the two dimensional space) of the M transmitters, and by (rx_l, ry_l) , $l = 1, \dots, N$ the locations of the N receivers.

¹Angular spread is the target's radar cross section variability as a function of aspect ratio.

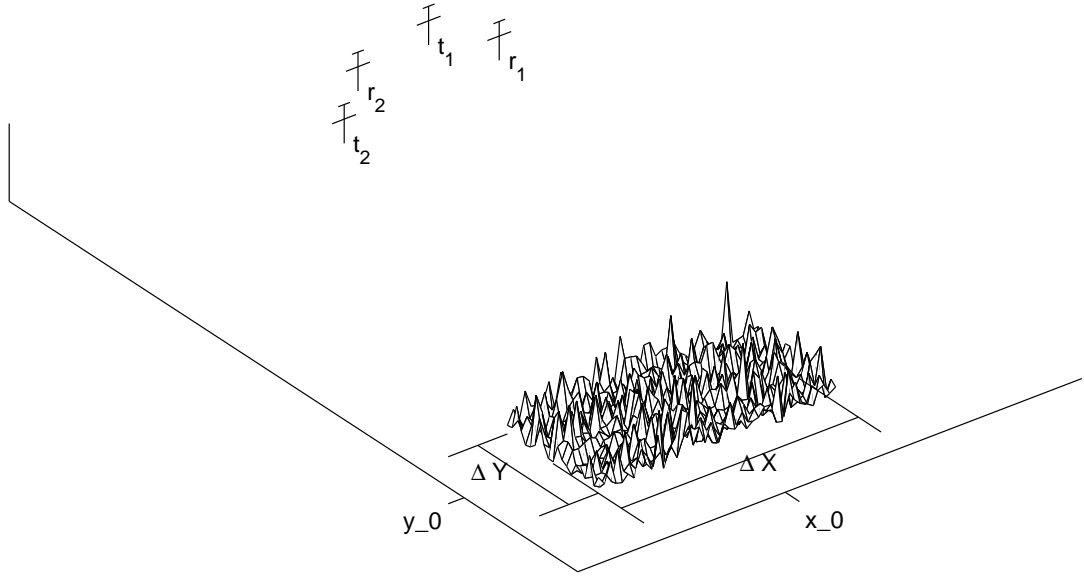


Fig. 1. Spatial Configuration

In the figure, t_1 and t_2 represent transmitters, while r_1 and r_2 represent receivers.

We assume that the target is composed of an infinite number of random, isotropic and independent scatterers, uniformly distributed over $[x_0 - \frac{\Delta x}{2}, x_0 + \frac{\Delta x}{2}] \times [y_0 - \frac{\Delta y}{2}, y_0 + \frac{\Delta y}{2}]$. Denote by $\Sigma(x, y)$ the complex gain of the scatterer located at $(x + x_0, y + y_0)$, for $(x, y) \in [-\frac{\Delta x}{2}, \frac{\Delta x}{2}] \times [-\frac{\Delta y}{2}, \frac{\Delta y}{2}]$. We model $\Sigma(x, y)$ as a zero mean, white, complex random variable, and $E\{|\Sigma(x, y)|^2\} = \frac{1}{\Delta x \Delta y}$. The last assumption is responsible for normalizing to one the average energy returned from the target.

In order to describe the received signal model, we need the following definitions: Denote by $d(x, y, x', y') \triangleq \sqrt{(x - x')^2 + (y - y')^2}$ be the distance between (x, y) and (x', y') . Let $\tau(x, y, x', y') \triangleq \frac{d(x, y, x', y')}{c}$ the time it takes a signal transmitted from (x, y) to reach (x', y') , where c is the speed of light. Assume that a narrow-band signal, denoted by $\sqrt{\frac{E}{M}} s_k(t)$, is transmitted from the k th transmitter, where $\|s_k(t)\|^2 = 1$ and E is the total average received energy. The received signal at the l th receiver is the superposition of the signals reflected from all the scatterers. Denote by $r_{lk}(t)$ the received signal at the l th receiver due to the signal transmitted from the k th transmitter, where $r_{lk}(t)$ obeys

$$r_{lk}(t) = \int_{x_0 - \frac{\Delta x}{2}}^{x_0 + \frac{\Delta x}{2}} \int_{y_0 - \frac{\Delta y}{2}}^{y_0 + \frac{\Delta y}{2}} \sqrt{\frac{E}{M}} s_k(t - \tau(tx_k, ty_k, \gamma, \beta) - \tau(rx_l, ry_l, \gamma, \beta)) \Sigma(\gamma - x_0, \beta - y_0) d\gamma d\beta$$

A change of variables $\beta + x_0 \rightarrow \beta$ and $\gamma + y_0 \rightarrow \gamma$ results in the following expression for $r_{lk}(t)$:

$$r_{lk}(t) = \int_{-\frac{\Delta x}{2}}^{\frac{\Delta x}{2}} \int_{-\frac{\Delta y}{2}}^{\frac{\Delta y}{2}} \sqrt{\frac{E}{M}} s_k(t - \tau(tx_k, ty_k, x_0, y_0) - (\tau(tx_k, tx_k, x_0 + \gamma, y_0 + \beta) - \tau(tx_k, ty_k, x_0, y_0)) - \tau(rx_l, ry_l, x_0, y_0) - (\tau(rx_l, ry_l, x_0 + \gamma, y_0 + \beta) - \tau(rx_l, ry_l, x_0, y_0))) \Sigma(\gamma, \beta) d\gamma d\beta$$

Invoking the narrowband assumption:

$$r_{lk}(t) = \sqrt{\frac{E}{M}} s_k(t - \tau(tx_k, ty_k, x_0, y_0) - \tau(rx_l, ry_l, x_0, y_0)) \int_{-\frac{\Delta x}{2}}^{\frac{\Delta x}{2}} \int_{-\frac{\Delta y}{2}}^{\frac{\Delta y}{2}} e^{-j2\pi f_c(\tau(tx_k, ty_k, x_0 + \gamma, y_0 + \beta) - \tau(tx_k, tx_k, x_0, y_0) + \tau(rx_l, ry_l, x_0 + \gamma, y_0 + \beta) - \tau(rx_l, ry_l, x_0, y_0))} \Sigma(\gamma, \beta) d\gamma d\beta \quad (1)$$

where f_c is the carrier frequency. This model can be further simplified by using the following approximations,

$$\begin{aligned} & \tau(tx_k, ty_k, x_0 + \gamma, y_0 + \beta) - \tau(tx_k, ty_k, x_0, y_0) \\ &= \frac{\sqrt{(tx_k - (x_0 + \gamma))^2 + (ty_k - (y_0 + \beta))^2} - \sqrt{(tx_k - x_0)^2 + (ty_k - y_0)^2}}{c} \\ &= \frac{\sqrt{(tx_k - x_0)^2 + \gamma^2 + 2\gamma(tx_k - x_0) + (ty_k - y_0)^2 + \beta^2 + 2\beta(ty_k - y_0)} - \sqrt{(tx_k - x_0)^2 + (ty_k - y_0)^2}}{c} \\ &\approx \frac{\sqrt{(tx_k - x_0)^2 + 2\gamma(tx_k - x_0) + (ty_k - y_0)^2 + 2\beta(ty_k - y_0)} - \sqrt{(tx_k - x_0)^2 + (ty_k - y_0)^2}}{c} \\ &\approx \frac{\sqrt{(tx_k - x_0)^2 + (ty_k - y_0)^2} + \frac{\beta(tx_k - x_0) + \gamma(ty_k - y_0)}{\sqrt{(tx_k - x_0)^2 + (ty_k - y_0)^2}} - \sqrt{(tx_k - x_0)^2 + (ty_k - y_0)^2}}{c} \\ &= \frac{\beta(tx_k - x_0) + \gamma(ty_k - y_0)}{c\sqrt{(tx_k - x_0)^2 + (ty_k - y_0)^2}} k = \frac{\beta(tx_k - x_0) + \gamma(ty_k - y_0)}{c \cdot d(tx_k, ty_k, x_0, y_0)}, \end{aligned} \quad (2)$$

where the first approximation is due to the fact that $\gamma^2 + \beta^2 \ll (tx_k - x_0)^2 + (ty_k - y_0)^2$, and the second is due to $\sqrt{x + \epsilon} \approx \sqrt{x} + \frac{\epsilon}{2\sqrt{x}}$ for $\epsilon \ll x$.

By combining (1), and (2), and using the narrowband signal assumption, the received signal can be modeled as follows:

$$\begin{aligned} r_{lk}(t) &= \sqrt{\frac{E}{M}} s_k(t - \tau(tx_k, ty_k, x_0, y_0) - \tau(rx_l, ry_l, x_0, y_0)) \\ &\cdot \int_{-\frac{\Delta x}{2}}^{\frac{\Delta x}{2}} \int_{-\frac{\Delta y}{2}}^{\frac{\Delta y}{2}} e^{-2j\pi f_c \left(\frac{\beta(tx_k - x_0) + \gamma(ty_k - y_0)}{c \cdot d(tx_k, ty_k, x_0, y_0)} + \frac{\beta(rx_l - x_0) + \gamma(ry_l - y_0)}{c \cdot d(rx_l, ry_l, x_0, y_0)} \right)} \Sigma(\gamma, \beta) d\gamma d\beta \\ &= \alpha_{lk} \sqrt{\frac{E}{M}} s_k(t - \tau(tx_k, ty_k, x_0, y_0) - \tau(rx_l, ry_l, x_0, y_0)), \end{aligned} \quad (3)$$

where

$$\alpha_{lk} \triangleq \int_{-\frac{\Delta x}{2}}^{\frac{\Delta x}{2}} \int_{-\frac{\Delta y}{2}}^{\frac{\Delta y}{2}} e^{-2j\pi f_c \left(\frac{\beta(tx_k - x_0) + \gamma(ty_k - y_0)}{c \cdot d(tx_k, ty_k, x_0, y_0)} + \frac{\beta(rx_l - x_0) + \gamma(ry_l - y_0)}{c \cdot d(rx_l, ry_l, x_0, y_0)} \right)} \Sigma(\gamma, \beta) d\gamma d\beta. \quad (4)$$

Since $\Sigma(x, y)$ is a random field, α_{lk} is a random variable. The exact distribution of α_{lk} depends on the exact distribution of $\Sigma(x, y)$. However, due to the central limit theorem, α_{lk} is approximately a complex

normal random variable. The mean and variance of α_{lk} are given as follows:

$$E \{ \alpha_{lk} \} = \int_{-\frac{\Delta x}{2}}^{\frac{\Delta x}{2}} \int_{-\frac{\Delta y}{2}}^{\frac{\Delta y}{2}} e^{-2j\pi f_c \left(\frac{\beta(tx_k - x_0) + \gamma(ty_k - y_0)}{c \cdot d(tx_k, ty_k, x_0, y_0)} + \frac{\beta(rx_l - x_0) + \gamma(ry_l - y_0)}{c \cdot d(rx_l, ry_l, x_0, y_0)} \right)} E \{ \Sigma(\gamma, \beta) \} d\gamma d\beta = 0, \quad (5)$$

$$E \{ |\alpha_{lk}|^2 \} = \int_{-\frac{\Delta x}{2}}^{\frac{\Delta x}{2}} \int_{-\frac{\Delta y}{2}}^{\frac{\Delta y}{2}} \int_{-\frac{\Delta x}{2}}^{\frac{\Delta x}{2}} \int_{-\frac{\Delta y}{2}}^{\frac{\Delta y}{2}} e^{-j2\pi f_c \left(\frac{\beta(tx_k - x_0) + \gamma(ty_k - y_0)}{c \cdot d(tx_k, ty_k, x_0, y_0)} + \frac{\beta(rx_l - x_0) + \gamma(ry_l - y_0)}{c \cdot d(rx_l, ry_l, x_0, y_0)} - \frac{\eta(tx_k - x_0) + \zeta(ty_k - y_0)}{c \cdot d(tx_k, ty_k, x_0, y_0)} - \frac{\eta(rx_l - x_0) + \zeta(ry_l - y_0)}{c \cdot d(rx_l, ry_l, x_0, y_0)} \right)} E \{ \Sigma(\gamma, \beta) \Sigma^*(\eta, \zeta) \} d\gamma d\beta d\eta d\zeta = \int_{-\frac{\Delta x}{2}}^{\frac{\Delta x}{2}} \int_{-\frac{\Delta y}{2}}^{\frac{\Delta y}{2}} \frac{1}{\Delta x \Delta y} d\beta d\gamma = 1, \quad (6)$$

where we used the fact that $E \{ \Sigma(\gamma, \beta) \Sigma^*(\eta, \zeta) \} = \frac{1}{\Delta x \Delta y} \delta(\gamma - \eta) \delta(\beta - \zeta)$. Consequently, the distribution of α_{lk} can be approximated as $\alpha_{lk} \sim \mathcal{CN}(0, 1)$.

In order to write the received signal in compact-matrix form, we need additional notation. Let

$$\psi_k = 2\pi f_c (\tau(tx_k, ty_k, x_0, y_0) - \tau(tx_1, ty_1, x_0, y_0)) \quad (7)$$

$$\varphi_l = 2\pi f_c (\tau(rx_l, ry_l, x_0, y_0) - \tau(rx_1, ry_1, x_0, y_0)). \quad (8)$$

Since the signal is narrowband, $s(t - \tau(tx_k, ty_k, x_0, y_0) - \tau(rx_l, ry_l, x_0, y_0)) = e^{-j\psi_k - j\varphi_l} s(t - \tau(tx_1, ty_1, x_0, y_0) - \tau(rx_1, ry_1, x_0, y_0))$; and the received signal model, (3), can be further simplified as follows:

$$r_{lk}(t) = \alpha_{lk} e^{-j\psi_k - j\varphi_l} \sqrt{\frac{E}{M}} s_k(t - \tau(tx_1, ty_1, x_0, y_0) - \tau(rx_1, ry_1, x_0, y_0)). \quad (9)$$

The received signal at the l th receiver is the superposition of all the signals originating from the various transmitters plus the additive noise. Denote by $r_l(t)$ the received signal and by $n_l(t)$ the additive noise at the l th receiver, then $r_l(t)$ is given by the following model

$$r_l(t) = \sqrt{\frac{E}{M}} \sum_{k=1}^M \alpha_{lk} e^{-j\psi_k - j\varphi_l} s_k(t - \tau) + n_l(t), \quad (10)$$

where $\tau \triangleq \tau(tx_1, ty_1, x_0, y_0) - \tau(rx_1, ry_1, x_0, y_0)$.

Denote by $\mathbf{r}(t) = [r_1, \dots, r_N(t)]^T$ the collection of the received signals at the various receiving elements, and by $\mathbf{s}(t) = [s_1(t), \dots, s_M(t)]^T$ the collection of the transmitted signals from the various transmitting elements. The received signal vector can be described by the following simple model,

$$\mathbf{r}(t) = \sqrt{\frac{E}{M}} \text{diag}(\mathbf{a}(x_0, y_0)) \mathbf{H} \text{diag}(\mathbf{b}(x_0, y_0)) \mathbf{s}(t - \tau) + \mathbf{n}(t) \quad (11)$$

where \mathbf{H} is an $N \times M$ matrix, referred to as the channel matrix, such that $[\mathbf{H}]_{ji} = \alpha_{ji}$; $\text{diag}(\mathbf{v})$ is a diagonal matrix with \mathbf{v} on its diagonal; $\mathbf{a}(x_0, y_0) = [1, e^{i\varphi_2}, \dots, e^{i\varphi_N}]^T$ is a $N \times 1$ vector, which is a function of the target location, usually referred to as the receiver steering vector; $\mathbf{b}(x_0, y_0) = [1, e^{i\psi_2}, \dots, e^{i\psi_M}]^T$ is an $M \times 1$ vector, which is a function of the target location, usually referred to as the transmitter steering vector; and $\mathbf{n}(t) = [n_1(t), \dots, n_N(t)]^T$ is an $N \times 1$ vector representing the additive noise. We assume that

$\mathbf{n}(t)$ is a white, zero mean, complex normal random process with correlation matrix $\sigma_n^2 \mathbf{I}_N$, where \mathbf{I}_N is the $N \times N$ identity matrix.

In order to complete the received signal model, (11), we need to characterize the distribution of the channel matrix \mathbf{H} . As will be seen in the sequel, the exact distribution of the channel matrix depends on the distances between the array elements and the target. Different array-target configurations give rise to different channel matrix distributions. The MIMO² concept is related to one configuration; whereas the conventional model is related to another. Before we discuss these different configurations, we analyze the distribution of the channel matrix further.

We have already demonstrated that every element of the channel matrix \mathbf{H} is a zero mean, unit variance complex normal random variable. Denote by $\boldsymbol{\alpha} = [\alpha_{11}, \dots, \alpha_{1M}, \alpha_{21}, \dots, \alpha_{NM}]^T$ the vector that contains all the elements of the matrix \mathbf{H} . It is clear from our previous discussion that $\boldsymbol{\alpha}$ is complex normal random vector. Since the mean of each element of $\boldsymbol{\alpha}$ is zero, $\boldsymbol{\alpha} \sim \mathcal{CN}(\mathbf{0}_{MN}, \mathbf{R}_\alpha)$, where $\mathbf{0}_{MN}$ is the $MN \times 1$ all-zero vector, and $\mathbf{R}_\alpha = E\{\boldsymbol{\alpha}\boldsymbol{\alpha}^H\}$, (the superscript denotes conjugate transpose,) is the correlation matrix of the vector $\boldsymbol{\alpha}$. The matrix \mathbf{R}_α , depends on the exact arrays-target configuration. However, there exists several cases in which we can approximate \mathbf{R}_α using very simple expressions.

Consider α_{jk} and α_{jl} . The correlation between α_{jk} and α_{jl} is given by,

$$\begin{aligned}
E\{\alpha_{jk}\alpha_{jl}^*\} &= E\left\{\int_{-\frac{\Delta x}{2}}^{\frac{\Delta x}{2}} \int_{-\frac{\Delta y}{2}}^{\frac{\Delta y}{2}} \int_{-\frac{\Delta x}{2}}^{\frac{\Delta x}{2}} \int_{-\frac{\Delta y}{2}}^{\frac{\Delta y}{2}} e^{-2j\pi f_c \left(\frac{\beta(tx_k-x_0)+\gamma(ty_k-y_0)}{c \cdot d(tx_k, ty_k, x_0, y_0)} + \frac{\beta(rx_j-x_0)+\gamma(ry_j-y_0)}{d \cdot d(rx_j, ry_j, x_0, y_0)}\right)} \Sigma(\gamma, \beta) \right. \\
&\quad \cdot \left. e^{j\frac{2\pi}{\lambda_c} \left(\frac{\eta(tx_l-x_0)+\xi(ty_l-y_0)}{d(tx_l, ty_l, x_0, y_0)} + \frac{\eta(rx_j-x_0)+\xi(ry_j-y_0)}{d(rx_j, ry_j, x_0, y_0)}\right)} \Sigma(\eta, \xi) d\gamma d\beta d\eta d\xi \right\} \\
&= \int_{-\frac{\Delta x}{2}}^{\frac{\Delta x}{2}} \int_{-\frac{\Delta y}{2}}^{\frac{\Delta y}{2}} \int_{-\frac{\Delta x}{2}}^{\frac{\Delta x}{2}} \int_{-\frac{\Delta y}{2}}^{\frac{\Delta y}{2}} e^{-j\frac{2\pi}{\lambda_c} \left(\frac{\beta(tx_k-x_0)+\gamma(ty_k-y_0)}{d(tx_k, ty_k, x_0, y_0)} + \frac{\beta(rx_j-x_0)+\gamma(ry_j-y_0)}{d(rx_j, ry_j, x_0, y_0)} - \frac{\eta(tx_l-x_0)+\xi(ty_l-y_0)}{d(tx_l, ty_l, x_0, y_0)} - \frac{\eta(rx_j-x_0)+\xi(ry_j-y_0)}{d(rx_j, ry_j, x_0, y_0)}\right)} \\
&\quad \cdot E\{\Sigma(\gamma, \beta)\Sigma(\eta, \xi)\} d\gamma d\beta d\eta d\xi \\
&= \frac{1}{\Delta x \Delta y} \int_{-\frac{\Delta x}{2}}^{\frac{\Delta x}{2}} \int_{-\frac{\Delta y}{2}}^{\frac{\Delta y}{2}} e^{-j\frac{2\pi}{\lambda_c} \left(\frac{\beta(tx_k-x_0)+\gamma(ty_k-y_0)}{d(tx_k, ty_k, x_0, y_0)} + \frac{\beta(rx_j-x_0)+\gamma(ry_j-y_0)}{d(rx_j, ry_j, x_0, y_0)} - \frac{\beta(tx_l-x_0)+\gamma(ty_l-y_0)}{d(tx_l, ty_l, x_0, y_0)} - \frac{\beta(rx_j-x_0)+\gamma(ry_j-y_0)}{d(rx_j, ry_j, x_0, y_0)}\right)} d\gamma d\beta \\
&= \frac{1}{\Delta x} \int_{-\frac{\Delta x}{2}}^{\frac{\Delta x}{2}} e^{-j\frac{2\pi}{\lambda_c} \left(\frac{\beta(tx_k-x_0)}{d(tx_k, ty_k, x_0, y_0)} - \frac{\beta(tx_l-x_0)}{d(tx_l, ty_l, x_0, y_0)}\right)} d\beta \frac{1}{\Delta y} \int_{-\frac{\Delta y}{2}}^{\frac{\Delta y}{2}} e^{-j\frac{2\pi}{\lambda_c} \left(\frac{\gamma(ty_k-y_0)}{d(tx_k, ty_k, x_0, y_0)} - \frac{\gamma(ty_l-y_0)}{d(tx_l, ty_l, x_0, y_0)}\right)} d\gamma, \quad (12)
\end{aligned}$$

where we used the fact that $E\{\Sigma(x, y)\Sigma(u, v)\} = \frac{1}{\Delta x \Delta y} \delta(x-u)\delta(y-v)$.

In order to get further insight into $E\{\alpha_{jk}\alpha_{jl}^*\}$, we develop conditions under which $\left|E\{\alpha_{jk}\alpha_{jl}^*\}\right|$ is either approximately zero or approximately one. Define $d \triangleq \frac{d(tx_k, ty_k, x_0, y_0) + d(tx_l, ty_l, x_0, y_0)}{2}$, and $d' \triangleq \frac{d(tx_k, ty_k, x_0, y_0) - d(tx_l, ty_l, x_0, y_0)}{2}$, and consider,

$$\frac{1}{\Delta x} \int_{-\frac{\Delta x}{2}}^{\frac{\Delta x}{2}} e^{-j\frac{2\pi}{\lambda_c} \left(\frac{\beta(tx_k-x_0)}{\tau(tx_k, ty_k, x_0, y_0)} - \frac{\beta(tx_l-x_0)}{\tau(tx_l, ty_l, x_0, y_0)}\right)} d\beta = \frac{1}{\Delta x} \int_{-\frac{\Delta x}{2}}^{\frac{\Delta x}{2}} e^{-j\frac{2\pi}{\lambda_c} \frac{(d-d')(tx_k-x_0) - (d+d')(tx_l-x_0)}{(d-d')(d+d')}} \beta d\beta, \quad (13)$$

where λ_c is the carrier wavelength. It is easily seen that a sufficient condition for the above expression to be much less than one is that the integrand completes at least one cycle or equivalently $\frac{2\pi}{\lambda_c} \frac{(d-d')(tx_k-x_0) - (d+d')(tx_l-x_0)}{(d-d')(d+d')} \frac{\Delta x}{2} >$

²For readability, in the sequel, we shorten ‘‘statistical MIMO’’ to plain ‘‘MIMO’’.

π . Using some algebraic manipulations this condition can be reduced to

$$(tx_k - tx_l)(d - d') + 2d'x_0 > \lambda_c(d + d')(d - d')/\Delta x. \quad (14)$$

Without loss of generality, we can choose d' to have the same sign as x_0 , hence $2d'x_0 > 0$, and we can strengthen the inequality by requiring that

$$d' = (tx_k - tx_l) > \lambda_c(d + d')/\Delta x. \quad (15)$$

Condition (15) has a simple physical interpretation. The target is illuminated by the transmitter and it reflects the energy back. The target can be regarded as an antenna with aperture Δx and beamwidth $\lambda_c/\Delta x$. If two transmitters are not within the same receive beamwidth of the target, then they see different “aspects” of the target with uncorrelated RCSs. Our condition examines whether the two transmitters are separated by more than the angular spread of the target or not.

This simple condition, (15), allows us to determine whether the elements of the channel matrix \mathbf{H} are considered correlated or not. Consider, for example, the jk th and il th elements of the channel matrix \mathbf{H} . If at least one of the following four conditions

$$\begin{aligned} (1) \quad rx_j - rx_i &> d(rx_j, ry_j, x_0, y_0)\lambda_c/\Delta x, \\ (2) \quad tx_k - tx_l &> d(tx_k, ty_k, x_0, y_0)\lambda_c/\Delta x, \\ (3) \quad ry_j - ry_i &> d(rx_j, ry_j, x_0, y_0)\lambda_c/\Delta y, \\ (4) \quad ty_k - ty_l &> d(tx_k, ty_k, x_0, y_0)\lambda_c/\Delta y \end{aligned} \quad (16)$$

holds, the jk th and il th elements of the channel matrix are *uncorrelated*. Note that (16) is a sufficient condition.

In contrast to (16), we would like to develop a similar condition under which two elements of the channel matrix \mathbf{H} are deemed correlated. Based on the discussion so far, if the integrands in (13) do not complete more than, say, 10% of a cycle, the correlation between α_{jk} and α_{il} is close to one. It can be easily seen from (16) that if the following four conditions hold jointly

$$\begin{aligned} (1) \quad rx_j - rx_i &<< d(rx_j, ry_j, x_0, y_0)\lambda_c/\Delta x, \\ (2) \quad tx_k - tx_l &<< d(tx_k, ty_k, x_0, y_0)\lambda_c/\Delta x, \\ (3) \quad ry_j - ry_i &<< d(rx_j, ry_j, x_0, y_0)\lambda_c/\Delta y, \\ (4) \quad ty_k - ty_l &<< d(tx_k, ty_k, x_0, y_0)\lambda_c/\Delta y \end{aligned} \quad (17)$$

then the jk th and il th elements of the channel matrix are approximately *fully correlated*.

B. Model Classification

Our received signal model, (11), can be used to describe many different systems. These systems differ in two aspects: the correlation between the elements of the channel matrix \mathbf{H} and the design of the

transmitted signals. In this paper, we consider four canonical systems, which we believe represent the four extreme cases. These four systems are the conventional phased array radar, the MIMO radar, and the multiple input single output (MISO) and the single input multiple output (SIMO) radars. Each of these four canonical systems represents a large number of similar systems. Consequently, it is sufficient to examine these systems in order to compare which one is preferable and where.

B.1 Phased Array Radar

Phased array radars are probably the most common radar systems that use an array of sensors. Phased array radars utilizes on an array of closely spaced sensors. That is, every pair of elements obeys condition (17). In addition, in phased array radar the transmitted signal is given by $\mathbf{s}(t) = \tilde{\mathbf{b}}s(t)$, where $\tilde{\mathbf{b}}$ is usually referred to as the transmitter steering vector.

When every pair of elements obeys condition (17), all the elements of the channel matrix are fully correlated. Therefore, the channel matrix is given by $\alpha \mathbf{1}_{NM}$, where $\alpha \sim \mathcal{CN}(0, 1)$, and $\mathbf{1}_{NM}$ is the $N \times M$ all-ones matrix. Particularizing the received signal model, (11), to this case, results in the following received signal,

$$\mathbf{r}(t) = \sqrt{\frac{E}{M}} \alpha \mathbf{a}(x_0, y_0) \mathbf{b}(x_0, y_0)^H \tilde{\mathbf{b}} s(t - \tau) + \mathbf{n}(t). \quad (18)$$

In phase array radar systems, both $\mathbf{a}(x_0, y_0)$ and $\mathbf{b}(x_0, y_0)$ are functions of the angle between the array and the target. It is common to denote these steering vectors by $\mathbf{a}(\theta)$ and $\mathbf{b}(\theta')$ respectively, where θ (θ') is the angle between the receiving (transmitting) array and the target. If, in addition, the receiver uses a beamformer to steer towards directions $\tilde{\theta}$, and the transmitter steering vector $\tilde{\mathbf{b}} = \mathbf{b}(\theta')$, then the output of the beamformer is

$$r(t) = \mathbf{a}(\tilde{\theta})^H \mathbf{r}(t) = \sqrt{\frac{E}{M}} \alpha \mathbf{a}(\tilde{\theta})^H \mathbf{a}(\theta) \mathbf{b}(\theta')^H \mathbf{b}(\tilde{\theta}) s(t - \tau) + n(t). \quad (19)$$

This model represents a bistatic radar where $\mathbf{b}(\theta')^H \mathbf{b}(\tilde{\theta})$ plays the role of the transmit antenna pattern, and $\mathbf{a}(\theta)^H \mathbf{a}(\tilde{\theta})$ is the receive antenna pattern. Since $n(t) = \mathbf{a}(\tilde{\theta})^H \mathbf{n}(t)$ is a linear transformation of $\mathbf{n}(t)$, $n(t)$ is a zero mean, complex normal random process with correlation function $\|\mathbf{a}(\tilde{\theta})\|^2 \sigma_n^2 \delta(\tau) = N \sigma_n^2 \delta(\tau)$.

In phased array radar, a processing gain of NM can be realized by taking $\theta = \tilde{\theta}$ and $\theta' = \tilde{\theta}'$, $\mathbf{a}(\tilde{\theta})^H \mathbf{a}(\theta) = N$, and $\mathbf{b}(\tilde{\theta}')^H \mathbf{b}(\theta) = M$. This processing gain does not come free of cost. Phased array radars are sensitive to the distribution of the fading coefficient α . If it happens that α is small, there is no way to overcome this fade, and the target will not be detected, or the estimation error will be large. MIMO radars are capable of overcoming this exact problem by exploiting spatial diversity.

The radars proposed in [15] has been referred to by the authors as MIMO radars. In these radars each transmitter transmits one of M orthogonal waveforms. It was shown in [15] that with proper processing, phased array radar that use this type of signaling can realize a coherent processing gain of N . However,

since the transmitted signals are orthogonal, this radar has a low probability of intercept (LPI). According to our classification these radars belong to the phased array category.

B.2 MIMO Radar

While in phased array radar, the inter-element spacing between every pair of elements obeys condition (17), in MIMO radar the inter-element spacings between each pair of elements obeys condition (16). Therefore, all the elements of the channel matrix are uncorrelated, that is $\boldsymbol{\alpha} \sim \mathcal{CN}(0, \mathbf{I}_{MN})$. Particularizing the received signal model, (11), to this case results in the following model,

$$\mathbf{r}(t) = \sqrt{\frac{E}{M}} \mathbf{H} \mathbf{s}(t - \tau) + \mathbf{n}(t). \quad (20)$$

With MIMO radar, each transmitter-receiver pair sees a different aspect of the target. In particular, by proper selection of the transmitted signals from the various transmitters, one can generate the equivalent of MN radar systems.

Assume that each of the M transmitters transmits one of M orthogonal signals, and denote these signals by $s_i(t)$, $i = 1, \dots, M$. By matched filtering each of the elements of $\mathbf{r}(t)$ with each of the transmitted signals, we can reconstruct $r_{ji}(t) = \sqrt{\frac{E}{M}} \alpha_{ji} s_i(t - \tau) + n_{ji}(t)$, where $n_{ji}(t)$ is a zero mean, complex normal random process with correlation function $R_n(\tau) = \sigma_n^2 \delta(\tau)$.

While in conventional radar the processing gain is MN and the radar sees only single aspect of the target, in MIMO radar, there is no coherent processing gain, but we synthesize MN independent radars. As a result, MIMO radar overcomes deep fades.

B.3 MISO and SIMO radar

In conventional radar, all the inter-element spacings are small; whereas in MIMO radar, elements are widely spaced. It is sometime desirable to mix these two approaches. MISO and SIMO radars are a compromise between phased array radars and MIMO radars. In MISO radar, the inter-element spacings of the transmitting elements obey (16), while the inter-element spacings of the receiving elements obey (17). In contrast, in SIMO radar, the inter-element spacings of the transmitting elements obey (17), while the inter-element spacings of the receiving elements obey (16). In what follows we concentrate on the MISO radars, and we omit the discussion on SIMO radars due to space limitations.

Since every pair of transmitting elements obeys (16), α_{ji} and α_{kl} are uncorrelated for $i \neq l$. However, since every pair of receiving elements obeys (17), α_{ji} and α_{ki} are fully correlated. Therefore, the channel matrix, \mathbf{H} , equals $\mathbf{1}_N \boldsymbol{\alpha}^H$, where $\boldsymbol{\alpha} \sim \mathcal{CN}(0, \mathbf{I}_M)$, and $\mathbf{1}_N$ is the all ones vector of length N . Particularizing the received signal model, (11) to this case results in the following model,

$$\mathbf{r}(t) = \sqrt{\frac{E}{M}} \mathbf{a}(\theta) \boldsymbol{\alpha}^H \mathbf{s}(t - \tau) + \mathbf{n}(t). \quad (21)$$

MISO radar can realize a coherent processing gain of $\|\mathbf{a}(\theta)\|^2 = N$ and create M independent radars. To see this, suppose that, as in MIMO radar, each of the M transmitters transmits one of M orthogonal

signals, $s_i(t)$ ($i = 1, \dots, M$). The receiver first steers toward θ , and then uses a beamformer to combine the received signal vectors. By matched filtering the beamformed signal we can construct the following M signals, $r_i(t) = N\sqrt{\frac{E}{M}}\alpha_i s_i(t - \tau) + n_i(t)$, where $n_i(t)$ is a zero mean, complex normal random process with correlation function $R_n(\tau) = N\sigma_n^2\delta(\tau)$. A complete analysis of MISO radars and their application for direction finding can be found in [22].

III. BASIC PERFORMANCE COMPARISONS

The radar detection problem can be formulated as follows [17]:

$$\begin{aligned} \mathcal{H}_0 &: \text{Target does not exist at delay } \tau \\ \mathcal{H}_1 &: \text{Target exists at delay } \tau. \end{aligned} \quad (22)$$

Many variants of this basic detection problem have been investigated and analyzed in the past. These variants differ by the assumed signal model, the unknown parameters, etc. In this section, we investigate the best achievable performance with phased array, MIMO, and MISO radars. We then compare the various systems and determine the optimal one.

Since we are interested in the inherent limitations of the various systems, in this section, we assume that θ , θ' , and the noise level, σ_n^2 , are all known in advance. The optimal, in the Neyman-Pearson sense, detector is the Likelihood Ratio Test (LRT), which is given by [23],

$$T = \log \frac{f(\mathbf{r}(t)|\mathcal{H}_1)}{f(\mathbf{r}(t)|\mathcal{H}_0)} \underset{<_{\mathcal{H}_0}}{\overset{>_{\mathcal{H}_1}}{\delta}}, \quad (23)$$

where $f(\mathbf{r}(t)|\mathcal{H}_0)$ and $f(\mathbf{r}(t)|\mathcal{H}_1)$ are the probability density functions (pdf) of the observation vector given the null and alternate hypotheses, respectively, and δ is a threshold, set by the desired probability of false alarm.

A. MIMO Radar

The following Lemma determines the structure of the MIMO radar's LRT detector.

Lemma 1: Denote by \mathbf{x} the $NM \times 1$ vector such that $[\mathbf{x}]_{iN+j} \triangleq \int r_i(t)s_j(t - \tau)dt$, that is, \mathbf{x} is the output of a bank of matched filters. The optimal detector is given by

$$T = \|\mathbf{x}\|^2 \underset{<_{\mathcal{H}_0}}{\overset{>_{\mathcal{H}_1}}{\delta}}, \quad (24)$$

where δ is set to ensure the required probability of false alarm.

Proof of Lemma 1: See Appendix A.

Notice the non-coherent nature of the MIMO radars detector.

It is easy to verify that \mathbf{x} is distributed as follows:

$$\mathbf{x} = \begin{cases} \mathbf{n} & \mathcal{H}_0 \\ \sqrt{\frac{E}{M}}\boldsymbol{\alpha} + \mathbf{n} & \mathcal{H}_1 \end{cases}, \quad (25)$$

where $\mathbf{n} \sim \mathcal{CN}(0, \sigma_n^2 \mathbf{I}_{MN})$ and $\boldsymbol{\alpha} \sim \mathcal{CN}(0, \mathbf{I}_{NM})$. Therefore, \mathbf{x} is a zero mean complex random variable with correlation matrix $\sigma_n^2 \mathbf{I}_{MN}$ under the null hypothesis, and $(\frac{E}{M} + \sigma_n^2) \mathbf{I}_{MN}$ under the alternate hypothesis. This leads to the following distribution of the test statistic,

$$\|\mathbf{x}\|^2 \sim \begin{cases} \frac{\sigma_n^2}{2} \chi_{(2MN)}^2 & \mathcal{H}_0 \\ \left(\frac{E}{2M} + \frac{\sigma_n^2}{2}\right) \chi_{(2MN)}^2 & \mathcal{H}_1 \end{cases}, \quad (26)$$

where $\chi_{(d)}^2$ denotes a chi-square random variable with d degrees of freedom.

It is well known that the probability of false alarm, the probability of detection, and the threshold are all connected by a series of one-to-one relations. These relations can be written with the aid of (26). The probability of false alarm can be expressed

$$\Pr_{FA} = \Pr(T > \delta | \mathcal{H}_0) = \Pr\left(\frac{\sigma_n^2}{2} \chi_{2MN}^2 > \delta\right) = \Pr\left(\chi_{2MN}^2 > \frac{2\delta}{\sigma_n^2}\right). \quad (27)$$

It follows that δ is set using the following formula,

$$\delta = \frac{\sigma_n^2}{2} F_{\chi_{2MN}^2}^{-1}(1 - \Pr_{FA}), \quad (28)$$

where $F_{\chi_{2MN}^2}^{-1}$ denotes the inverse cumulative distribution function of a chi-square random variable with $2MN$ degrees of freedom. The probability of detection is given by,

$$\begin{aligned} \Pr_D &= \Pr(T > \delta | \mathcal{H}_1) = \Pr\left(\left(\frac{E}{2M} + \frac{\sigma_n^2}{2}\right) \chi_{2MN}^2 > \delta\right) = 1 - F_{\chi_{2M}^2}\left(\frac{2\delta}{\frac{E}{M} + \sigma_n^2}\right) \\ &= 1 - F_{\chi_{2MN}^2}\left(\frac{\sigma_n^2}{\frac{E}{M} + \sigma_n^2} F_{\chi_{2MN}^2}^{-1}(1 - \Pr_{FA})\right). \end{aligned} \quad (29)$$

It is interesting to note that both the test statistic, (24), and the threshold, (28), are independent of the transmitted energy E . Therefore, the optimal detector, even in the case of unknown signal energy, is given by (24) and (28). This establishes the fact that (24) is a Uniformly Most Powerful (UMP) detector for which only the noise level needs to be known [24].

B. Phased Array Radar

Consider a phased array radar system. The following lemma describes the structure of the phased array LRT Detector,

Lemma 2: Let $x = \int \mathbf{r}^H(t) \mathbf{a}(\theta) s(t - \tau) dt$ be the output of the spatial-temporal matched filter. The optimal detector is given by

$$T = |x|^2 \underset{\mathcal{H}_0}{\overset{\mathcal{H}_1}{>}} \delta \quad (30)$$

where δ is set to ensure the required probability of false alarm is achieved.

Proof of Lemma 2: See Appendix B.

The optimal detector for the phased array system turns out to be the beamformer steering to direction θ followed by a simple linear filter (also known as the Echardt filter) [25]. It is interesting to note that the optimal detector, whether target fading exists or not, is the same.

The optimal detector is independent of the transmitter steering vector, $\tilde{\mathbf{b}}$, used. Optimizing this vector will result in the optimal phased array system. It is easy to see that x is described by the following model,

$$x = \begin{cases} n & \mathcal{H}_0 \\ \sqrt{\frac{E}{M}} \|\mathbf{a}(\theta)\|^2 \tilde{\mathbf{b}}^H \mathbf{b}(\theta') \alpha + n & \mathcal{H}_1 \end{cases}, \quad (31)$$

where $\alpha \sim \mathcal{CN}(0, 1)$ and $n \sim \mathcal{CN}(0, \sigma_n^2 \|\mathbf{a}(\theta)\|^2)$. This gives rise to the following distribution of the test statistic,

$$T \sim \begin{cases} \frac{\sigma_n^2 \|\mathbf{a}(\theta)\|^2}{2} \chi_{(2)}^2 & \mathcal{H}_0 \\ \left(\frac{\sigma_n^2 \|\mathbf{a}(\theta)\|^2}{2} + \frac{E \|\mathbf{a}(\theta)\|^4 |\tilde{\mathbf{b}}^H \mathbf{b}(\theta')|^2}{2M} \right) \chi_{(2)}^2 & \mathcal{H}_1 \end{cases}. \quad (32)$$

The probability of false alarm, the probability of detection, and the threshold can be easily derived using the same derivation leading respectively, to (27), (28), and (29). The probability of false alarm, the probability of detection, and the threshold are, respectively, given by,

$$\Pr_{FA} = \Pr \left(\chi_{(2)}^2 > \frac{2\delta}{\sigma_n^2 \|\mathbf{a}(\theta)\|^2} \right), \quad (33)$$

$$\delta = \frac{\sigma_n^2 \|\mathbf{a}(\theta)\|^2}{2} F_{\chi_2^2}^{-1} (1 - \Pr_{FA}), \quad (34)$$

$$\Pr_D = 1 - F_{\chi_2^2} \left(\frac{\sigma_n^2}{\left(\sigma_n^2 + \frac{E \|\mathbf{a}(\theta)\|^2 |\tilde{\mathbf{b}}^H \mathbf{b}(\theta')|^2}{M} \right)} F_{\chi_2^2}^{-1} (1 - \Pr_{FA}) \right). \quad (35)$$

Since the cumulative distribution function $F_{\chi_2^2}(\cdot)$ is a monotonic increasing function, the probability of detection is maximized when the argument of (35) is minimized. This in turn happens when $|\tilde{\mathbf{b}}^H \mathbf{b}(\theta')|^2$ is maximized. Using the Cauchy-Schwartz inequality, $|\tilde{\mathbf{b}}^H \mathbf{b}(\theta')|^2$ is maximized when $\tilde{\mathbf{b}} = \mathbf{b}(\theta')$. Substituting the optimal $\tilde{\mathbf{b}}$ into (35) results in the following expression for the probability of detection,

$$\Pr_D = 1 - F_{\chi_2^2} \left(\frac{\sigma_n^2}{\left(\sigma_n^2 + \frac{E \|\mathbf{a}(\theta)\|^2 \|\mathbf{b}(\theta')\|^4}{M} \right)} F_{\chi_2^2}^{-1} (1 - \Pr_{FA}) \right) = 1 - F_{\chi_2^2} \left(\frac{\sigma_n^2}{(\sigma_n^2 + ENM)} F_{\chi_2^2}^{-1} (1 - \Pr_{FA}) \right), \quad (36)$$

where we used the fact that $\|\mathbf{a}(\theta)\|^2 = N$ and $\|\mathbf{b}(\theta')\|^2 = M$.

C. MISO Radar

The last system we consider is the MISO radar. It is very easy to verify that MISO radar is a hybrid of both the MIMO and the phased array systems. Therefore, it should not be a surprise that the optimal detector is a combination of the corresponding optimal detectors. The following lemma describes the MISO radar's optimal detector.

Lemma 3: Denote by \mathbf{x} an $M \times 1$ vector such that $[\mathbf{x}]_i \triangleq \int \mathbf{r}^H(t) \mathbf{a}(\theta) s_i(t - \tau) dt$, that is, \mathbf{x} is the output of a bank of spatial-temporal matched filters. The optimal detector is then given by

$$T = \|\mathbf{x}\|^2 \underset{\mathcal{H}_0}{\overset{\mathcal{H}_1}{>}} \delta, \quad (37)$$

where δ is set to ensure the required probability of false alarm.

The proof of Lemma 3 is a simple modification of the proofs of Lemmas 1 and 2, and hence it is omitted. The receiving array is composed of closely spaced sensors. Consequently, the receiver can cohere a beam toward the target and coherently combine the signals received at the receiving array. However, the spatially combined signal contains several orthogonal signals sent from different antennas. The optimal detector de-spreads these orthogonal signals. Since these signals arrive with unknown gains and phases, the detector combines these signals non-coherently, the same way the MIMO radar does.

The probability of false alarm and the probability of detection can be computed from (27), (29), (33), and (36), and they are given respectively by

$$\Pr_{FA} = \Pr \left(\chi_{(2M)}^2 > \frac{2\delta}{\sigma_n^2 \|\mathbf{a}(\theta)\|^2} \right), \quad (38)$$

$$\delta = \frac{\sigma_n^2 \|\mathbf{a}(\theta)\|^2}{2} F_{\chi_{2M}^2}^{-1} (1 - \Pr_{FA}), \quad (39)$$

$$\Pr_D = 1 - F_{\chi_{2M}^2} \left(\frac{\sigma_n^2}{(\sigma_n^2 + \frac{EN}{M})} F_{\chi_{2M}^2}^{-1} (1 - \Pr_{FA}) \right). \quad (40)$$

D. Discussion

The most useful performance measure of any detector is its probability of detection. Therefore, we should compare the probability of detection of the various systems in order to determine the best. We will do this comparison based on numerical examples in the next section. Another approach, which is analytically tractable, is to compare the various systems based on a single scalar performance measure. Such a performance measure should summarize the detector performance in a single number instead of a function. One such performance measure is the detector's signal-to-noise ratio (SNR) (also referred to as divergance in [26]).

Let T be some test statistic (detector). The detector's SNR, denoted by β , is defined as follows:

$$\beta = \frac{|E(T|\mathcal{H}_0) - E(T|\mathcal{H}_1)|^2}{\frac{1}{2} [\text{Var}(T|\mathcal{H}_0) + \text{Var}(T|\mathcal{H}_1)]}. \quad (41)$$

If $T|\mathcal{H}_i$, $i = 0, 1$ is normally distributed, $\sqrt{\beta}$ represents the normalized distance between the means of the distribution of the detector's test statistics under the null and alternate hypotheses. This in turn represents our ability to distinguish between the two hypotheses. Although, in our problem, $T|\mathcal{H}_i$ is not normally distributed, we find this measure very useful in capturing the detector's performance in one simple number.

Consider a MIMO radar system. According to (26), $E(T|\mathcal{H}_0) = MN\sigma_n^2$, and $E(T|\mathcal{H}_1) = MN\sigma_n^2 + NE$, and hence $|E(T|\mathcal{H}_0) - E(T|\mathcal{H}_1)|^2 = N^2E^2$. Also, according to (26), $\text{Var}(T|\mathcal{H}_0) = MN\sigma_n^4$, and

$\text{Var}(T|\mathcal{H}_1) = MN(E^2/M^2 + 2E\sigma_n^2 + \sigma_n^4)$, and hence $[\text{Var}(T|\mathcal{H}_0) + \text{Var}(T|\mathcal{H}_1)] = MN(E^2/M^2 + 2E\sigma_n^2/M + 2\sigma_n^4)$. Combining these results, we obtain the following detector SNR

$$\beta_{MIMO} = \frac{E^2 N^2}{MN(E^2/2M^2 + \sigma_n^4 + E\sigma_n^2/M)} = \frac{E^2 N}{M(E^2/2M^2 + \sigma_n^4 + E\sigma_n^2/M)}. \quad (42)$$

Define the SNR, denoted by ρ , as the ratio between the total transmitted energy and the noise level per receive element, that is $\rho \triangleq E/\sigma_n^2$. The detector SNR can be further simplified and is given by the following expression,

$$\beta_{MIMO} = \frac{\rho^2 N}{M(1 + \rho^2/2M^2 + \rho/M)}. \quad (43)$$

Now consider a phased array radar system. According to (32), $E(T|\mathcal{H}_0) = N\sigma_n^2$, and $E(T|\mathcal{H}_1) = N\sigma_n^2 + N^2ME$, and hence $|E(T|\mathcal{H}_0) - E(T|\mathcal{H}_1)|^2 = N^4M^2E^2$. Also, according to (32), $\text{Var}(T|\mathcal{H}_0) = N^2\sigma_n^4$, and $\text{Var}(T|\mathcal{H}_1) = N^2\sigma_n^4 + E^2N^4M^2 + 2\sigma_n^2EN^3M$, and hence $[\text{Var}(T|\mathcal{H}_0) + \text{Var}(T|\mathcal{H}_1)] = 2N^2\sigma_n^4 + E^2N^4M^2 + 2\sigma_n^2EN^3M$. The SNR of the optimal detector for the phased array radar system is given by the following expression,

$$\begin{aligned} \beta_{\text{phased array}} &= \frac{N^4M^2E^2}{\frac{1}{2}[2N^2\sigma_n^4 + E^2N^4M^2 + 2\sigma_n^2EN^3M]} = \frac{N^2M^2E^2}{\frac{1}{2}[2\sigma_n^4 + E^2N^2M^2 + 2\sigma_n^2EMN]} \\ &= \frac{N^2M^2\rho^2}{1 + M^2N^2\rho^2/2 + N\rho M}. \end{aligned} \quad (44)$$

Consider now a MISO system. The SNR of the optimal detector for a MISO is given by the following expression (a complete derivation is omitted due to space limitations),

$$\beta_{MISO} = \frac{E^2N^4}{\frac{1}{2}[2\sigma_n^4N^2M + 2N^3E\sigma_n^2 + \frac{E^2N^4}{M}]} = \frac{\rho^2N^2}{M + \rho^2N^2/M + N\rho} = \frac{\rho^2N^2}{M(1 + \rho^2N^2/2M^2 + N\rho/M)} \quad (45)$$

Figures 2 and 3 depict the optimal detectors' SNR for the phased array, MIMO, and MISO systems. In Figure 2, we assume $M = 1$ and $N = 4$, while in Figure 3, we assume that $M = N = 4$. It is evident from the figures that, while for high SNR, the MIMO system is optimal, for low SNR, the phased array system is optimal.

Assume that $\rho \gg 1$, that is high SNR. The optimal detectors' SNR can then be approximated as follows:

$$\beta_{MIMO} \approx 2NM, \quad \beta_{\text{phased array}} \approx 2, \quad \beta_{MISO} \approx 2M. \quad (46)$$

It is easily seen that in terms of its ability to distinguish between the two hypotheses, the MIMO radar is the best system, whereas the phased array system is the worst system. The received signal in a phased array system enjoys a coherent processing gain. However, the random gain due to target fluctuations, α , is Rayleigh distributed, and hence there is a non-negligible probability that α is either small or large. When α is small, although the transmitted power is high, the received power is low. Therefore, the received SNR is low with non-negligible probability. The MIMO radar system, on the other hand, is equivalent to

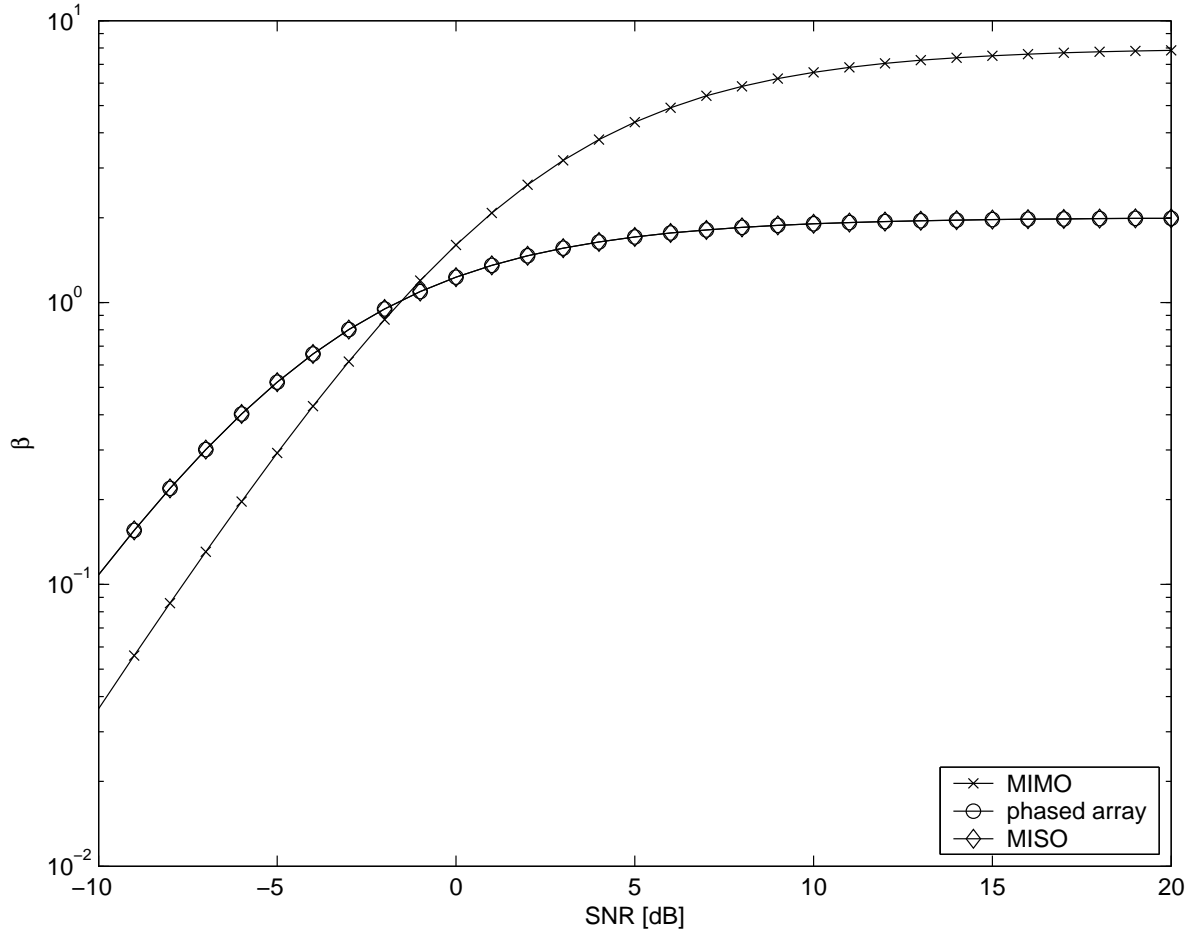


Fig. 2. The optimal detector's SNR in various systems. $M = 1$, $N = 4$. Note that the MISO and phased array curve fall on top of each other

NM independent radar systems, each of which is subject to Rayleigh distributed random gain. Since the number of independent radars is large, some of them are subject to deep fades, while others experience strong gains. However, the average received power does not vary considerably. Therefore, the MIMO radar is not subject to the deep fades that affect the phased array radar.

Assume that $\rho \ll 1$, that is low SNR. The optimal detectors' SNR can be approximated as follows:

$$\beta_{MIMO} \approx \rho^2 N/M, \quad \beta_{\text{phased array}} \approx \rho^2 N^2 M^2, \quad \beta_{MISO} \approx 2M. \quad (47)$$

For low SNR, the phased array radar system's disadvantage becomes its advantage. Since with non-negligible probability the random gain, α , is large, in those instances, the instantaneous SNR is high compared with the average SNR. Consequently, the target is detected by the phased array radar. On the other hand, the MIMO radar system does not enjoy this benefit. The received SNR can not deviate considerably from the average received SNR (recall that we have MN independent radars). Consequently, the probability of detection of the MIMO radar system is lower than that of the phased array system.

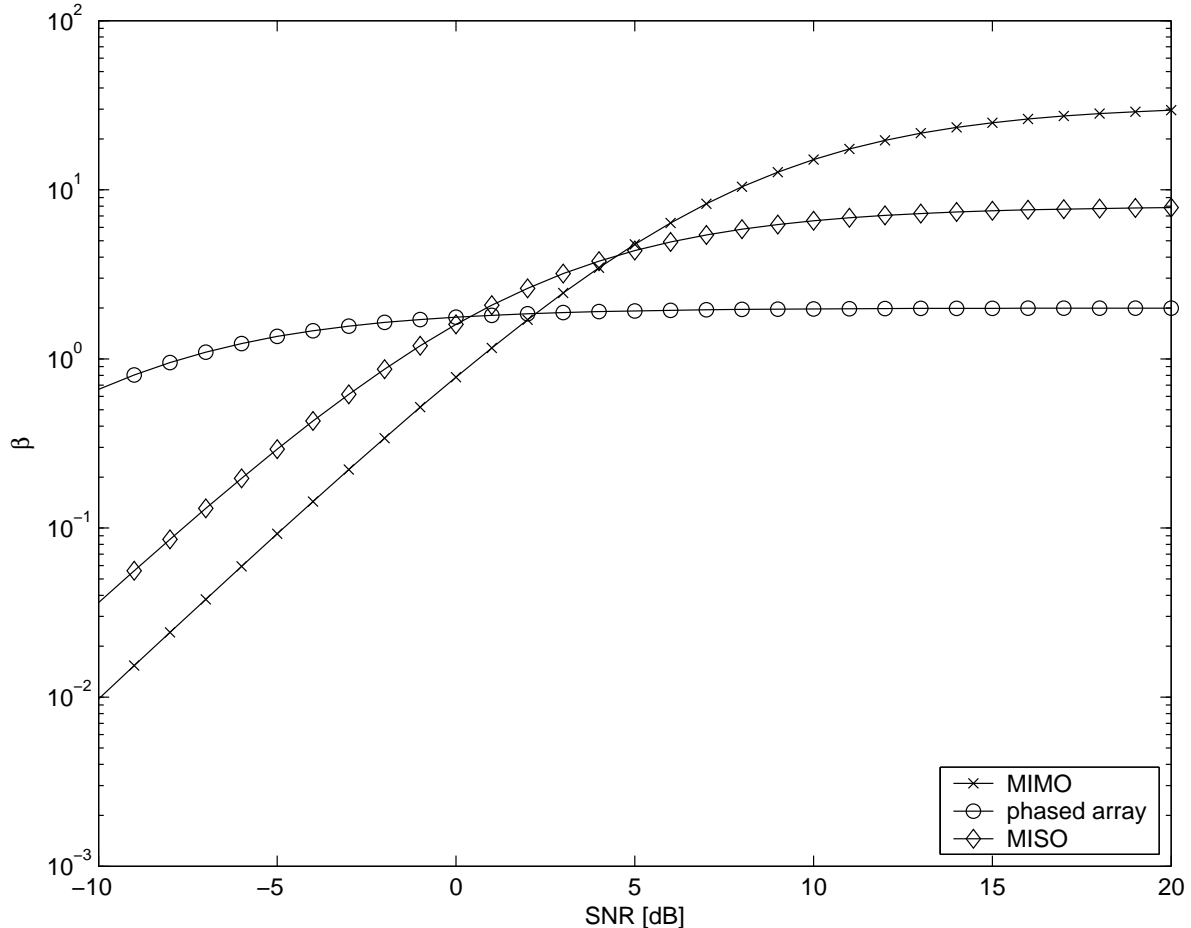


Fig. 3. The optimal detector's SNR in various systems. $M = N = 4$.

IV. THE OPTIMAL INVARIANT DETECTOR

In the previous section, we examined the performance of the optimal detector when all the parameters are known. This assumption is an unrealistic one, and usually both the noise level, σ_n^2 , and the transmitted power, E , are unknown. In real life systems, the noise level, σ_n^2 , depends on the clutter, and the transmitted power, E , includes implicitly the unknown target average radar cross section (RCS). Consequently, it is unrealistic to assume that either E or σ_n^2 are known in advance [4].

In radar theory there exist detectors that do not require explicit knowledge of either E or σ_n^2 . These detectors are usually constant-false-alarm-rate detectors (CFAR), and some of them are optimal in a very important sense [17]. In what follows, we derive the optimal detector for MIMO and MISO systems when both the noise level, σ_n^2 , and the transmitted energy, E , are unknown. We demonstrate that a very intuitive extension of the Mean Level Detector (MLD) is the optimal detector for MIMO radar systems in the invariant sense [27], [28].

When unknown parameters exist, many hypothesis testing problems do not possess an UMP detector. However, if we restrict our attention to a class of detectors having some special properties, e.g., CFAR, sometimes an optimal detector can be found. Usually these special properties are so natural that it is hard to imagine using a detector that does not possess these properties. The mathematical theory governing these special detectors is the theory of invariant decision rules. The theory of invariant decision rules is beyond the scope of this paper. (We refer the reader to [29], [24], [28] for an introduction to invariant hypothesis testing theory.) In order to enhance an intuitive understanding of the subject, we describe the mathematical theory of invariant decision rules in the context of our detection problem. We first formulate the exact detection problem when both the noise level and the average received power are unknown and then develop the optimal detector in the invariance sense.

A. Problem Formulation

In all the systems discussed so far, the output of the matched filter sampled at $t = \tau$ was a sufficient statistic. However, if both the noise level, σ_n^2 , and the average received power, E , are unknown, the information contained at the output of the matched filter sampled at $t = \tau$ is not sufficient for constructing a detector with bounded probability of false alarm. Take for example (25). Assume the null hypothesis, \mathcal{H}_0 , and that $\sigma_n^2 = 2$. The output of the matched filter sampled at $t = \tau$ is a zero mean, complex normal random vector with correlation matrix $2\mathbf{I}$. Assume, on the other hand, the alternate hypothesis, \mathcal{H}_1 , and that $\sigma_n^2 = 1$ and $E = M$. Again, the output of the matched filter sampled at $t = \tau$ is a zero mean, complex normal random vector with correlation matrix $2\mathbf{I}$. This simple example demonstrates that once both E and σ_n^2 are unknown, we can find one combination of the parameters that belongs to the null hypothesis, and another that belongs to the alternate hypothesis, that yield the same output of the matched filter sampled at $t = \tau$, i.e., the output is unidentifiable [30].

In order to overcome this problem, the common practice is to obtain additional samples of the noise process. This can be done, for example, by sampling the output of the matched filter in the vicinity of $t = \tau$. For a discussion on how to obtain these noise samples we refer the reader to [17]. Here we assume that L samples of the noise process were obtained by the receiver, and denote by $\mathbf{y} = [y_1, \dots, y_L]^T$ the $L \times 1$ vector that contains these samples, that is $\mathbf{y} \sim \mathcal{CN}(0, \sigma_n^2 \mathbf{I}_L)$.

Denote by \mathbf{x} the sufficient statistic when all the parameters are known, and by $l(\mathbf{x}) = |\mathbf{x}|$ the length of \mathbf{x} . In addition, denote by $\tilde{\mathbf{z}} \triangleq [\mathbf{y}^T, \mathbf{x}^T]^T$ the concatenation of \mathbf{y} and \mathbf{x} . It is easy to verify that independent of the exact system, e.g., phased array, MIMO, MISO, used,

$$\tilde{\mathbf{z}} \sim \mathcal{CN}(0, \text{diag}([\sigma_n^2 \mathbf{1}_{L \times 1}, (\sigma_n^2 + \mu) \mathbf{1}_{l(\mathbf{x}) \times 1}])) , \quad (48)$$

where μ depends on the system considered and whether or not a target exists. It can be easily shown that $\mathbf{z} = [||\mathbf{y}||^2, ||\mathbf{x}||^2]$ is a sufficient statistic for $\tilde{\mathbf{z}}$. Therefore, we will restrict our attention to \mathbf{z} instead

of $\tilde{\mathbf{z}}$. The sufficient statistic vector \mathbf{z} is distributed as follows,

$$\mathbf{z} \sim \left[\frac{\sigma_n^2}{2} \chi_{(2L)}^2, \frac{\sigma_n^2 + \mu}{2} \chi_{(2l(\mathbf{x}))}^2 \right]. \quad (49)$$

The detection problem can be formulated

$$\begin{aligned} \mathcal{H}_0 : \mu = 0, \sigma_n^2 \in \mathcal{R}_+ \\ \mathcal{H}_1 : \mu > 0, \sigma_n^2 \in \mathcal{R}_+, \end{aligned} \quad (50)$$

where \mathcal{R}_+ is the set of positive, real numbers.

This detection problem does not possess an UMP detector. However, it is only natural to restrict our attention to detectors that are invariant to scaling, that is, detectors, the performance of which depends only on the SNR and not on the actual noise level and average received signal energy. Moreover, if the structure of this detector is independent of the exact SNR, then the resulting detector is what is known as an UMP invariant detector.

B. Invariant Decision Rules and the Optimal Detector

In this section we provide a short introduction to invariant decision rules. We describe only the essential mathematical concepts without any specific proofs. After each step, we demonstrate the mathematical concept with our detection problem, (50).

Let \mathbf{Z} be a random vector whose pdf, denoted by $f_{\mathbf{Z}}(\mathbf{z}|\boldsymbol{\theta})$, $\boldsymbol{\theta} \in \Theta$, is known up to some unknown parameter vector, denoted by $\boldsymbol{\theta}$, belonging to a parameter space denoted by Θ . We denote by \mathbf{z} the observation vector, and by \mathcal{Z} the observation space. Assume that $\Theta = \Theta_0 \cup \Theta_1$ and $\Theta_0 \cap \Theta_1 = \emptyset$. We associate Θ_0 with the null hypothesis, and Θ_1 with the alternate hypothesis, that is, if \mathcal{H}_0 is true, $\boldsymbol{\theta} \in \Theta_0$, and if \mathcal{H}_1 is true, $\boldsymbol{\theta} \in \Theta_1$. In our detection problem $\boldsymbol{\theta} = [\sigma_n^2, \alpha]$ and $\Theta = \mathcal{R}_+^2$. In addition, $\Theta_0 = (\mathcal{R}_+, 0)$, and $\Theta_1 = (\mathcal{R}_+, \mathcal{R}_+ - \{0\})$.

Let \mathcal{G} denote a group of transformations from \mathbf{z} to \mathbf{z} . In addition, let the group operation be composition, that is, if $g_1, g_2 \in \mathcal{G}$, then $g \triangleq g_2 g_1$ is the transformation that takes \mathbf{z} to $g(\mathbf{z}) = g_2(g_1(\mathbf{z}))$.

Definition 1: The family of distributions $f_{\mathbf{Z}}(\mathbf{z}|\boldsymbol{\theta})$ is said to be invariant under the group \mathcal{G} , if for every $g \in \mathcal{G}$ and $\boldsymbol{\theta} \in \Theta$ there exists a unique $\boldsymbol{\theta}' \in \Theta$ such that $g(\mathbf{z})$ is distributed according to $f(\mathbf{z}|\boldsymbol{\theta}')$. Denote this $\boldsymbol{\theta}'$ by $\bar{g}(\boldsymbol{\theta})$. The interpretation is that g has left the pdf invariant in form, but the parameter $\boldsymbol{\theta}$ has changed to $\bar{g}(\boldsymbol{\theta})$.

Our main objective is to determine the optimal detector invariant to scaling, that is, the detector outcome when presented with both \mathbf{z} and $a\mathbf{z}$ should be the same. Using this in our problem, leads to $\mathcal{G} = \{g(\mathbf{z})|g(\mathbf{z}) = a\mathbf{z}, a \neq 0\}$. It is easy to verify that if $g(\mathbf{z}) = a\mathbf{z}$, then $\bar{g}(\boldsymbol{\theta}) = a\boldsymbol{\theta}$.

Definition 2: A group of transformations \mathcal{G} leaves a hypothesis-testing problem invariant if \mathcal{G} leaves both families of distributions $\{f(\mathbf{z}|\boldsymbol{\theta}), \boldsymbol{\theta} \in \Theta_0\}$ and $\{f(\mathbf{z}|\boldsymbol{\theta}), \boldsymbol{\theta} \in \Theta_1\}$ invariant.

It is easy to show that a hypothesis testing problem remains invariant if and only if $\bar{g}(\Theta_0) = \Theta_0$ and $\bar{g}(\Theta_1) = \Theta_1$. This condition expresses the requirement that the original dichotomy of Θ is maintained for any transformation g . The detection problem of (50) is an invariant hypothesis test problem. To see this, note that for every $\theta = (\sigma_n^2, 0) \in \Theta_0$, $\bar{g}(\theta) = (a^2\sigma_n^2, 0) \in \Theta_0$. Further, $\bar{g}(\Theta_0) \subseteq \Theta_0$. In addition, for every $\theta = (\sigma_n^2, 0) \in \Theta_0$, $\theta = \bar{g}(\theta/a^2)$, hence $\Theta_0 \subseteq \bar{g}(\Theta_0)$. Consequently, $\bar{g}(\Theta_1) = \Theta_1$.

A decision rule is a mapping of the observation space, \mathbf{z} , to the decision space $\{\mathcal{H}_0, \mathcal{H}_1\}$. We say that a decision rule $\phi : \mathbf{z} \rightarrow \{\mathcal{H}_0, \mathcal{H}_1\}$ is \mathcal{G} invariant if for all \mathbf{z} and $g \in \mathcal{G}$,

$$\phi(g(\mathbf{z})) = \phi(\mathbf{z}). \quad (51)$$

This condition reflects the requirement that the decision should be invariant to the group of transformations. For example, in our detection problem we require that whether we observe \mathbf{z} or $a\mathbf{z}$, the decision should be the same. This requirement is manifested in mathematical terms by equation (51). The definition of the invariant decision rule leads to the following definition:

Definition 3: A function $T(\mathbf{z})$ is said to be maximal invariant with respect to \mathcal{G} if (invariance) $T(g(\mathbf{z})) = T(\mathbf{z})$, $\forall \mathbf{z}$, and $\forall g \in \mathcal{G}$, and (maximality) $T(\mathbf{z}_1) = T(\mathbf{z}_2)$ implies $\mathbf{z}_1 = g(\mathbf{z}_2)$ for some $g \in \mathcal{G}$.

The interpretation of maximal invariant statistic is beyond the scope of this paper, and the interested reader is referred to [29].

It is easy to verify that a maximal invariant statistic for our detection problem is given by,

$$M(\mathbf{z}) = M(\|\mathbf{y}\|^2, \|\mathbf{x}\|^2) = \frac{\|\mathbf{x}\|^2}{\|\mathbf{y}\|^2}. \quad (52)$$

Theorem 1: A decision rule is \mathcal{G} -invariant if and only if it is a function of a maximal invariant statistic [24].

This theorem asserts that in searching for the optimal detector we can limit our search only to functions of $M(\mathbf{z})$ of (52).

The following theorem describes the optimal scale invariant detector for our detection problem:

Theorem 2: Consider the detection problem of (50). An UMP scale invariant (UMPI) detector exists and it given by

$$T = \frac{\|\mathbf{x}\|^2}{\|\mathbf{y}\|^2} \underset{<_{\mathcal{H}_0}}{>_{\mathcal{H}_1}} \delta. \quad (53)$$

Proof of Theorem 2: The proof of the theorem is divided into two parts. In the first part we will derive the optimal detector for two simple hypotheses and in the second we will demonstrate that the detector obtained in the first part is UMP.

Consider the following two simple hypotheses. Under the null hypothesis, the SNR is zero, while under the alternate hypothesis the SNR is a fixed value greater than zero. We are looking for the optimal invariant detector for deciding between these two hypothesis. According to Theorem 1 and the Neyman-Pearson Lemma, the optimal detector for this simple hypothesis testing problem is given by,

$$T = \frac{f(M(\mathbf{z})|\mathcal{H}_1)}{f(M(\mathbf{z})|\mathcal{H}_0)} \underset{<_{\mathcal{H}_0}}{>_{\mathcal{H}_1}} \delta. \quad (54)$$

The maximal invariant test statistic, $M(\mathbf{z})$, is the result of dividing two independent chi-squared random variables. Consequently,

$$M(\mathbf{z})|\mathcal{H}_0 \sim \frac{\chi_{(2l(\mathbf{x}))}^2}{\chi_{(2L)}^2} = \frac{l(\mathbf{x})}{L} \frac{\chi_{(2l(\mathbf{x}))}^2/2l(\mathbf{x})}{\chi_{(2L)}^2/2L} = \frac{l(\mathbf{x})}{L} \mathcal{F}_{2l(\mathbf{x}),2L} \quad (55)$$

$$M(\mathbf{z})|\mathcal{H}_1 \sim \frac{\sigma_n^2 + \mu}{\sigma_n^2} \frac{\chi_{(2l(\mathbf{x}))}^2}{\chi_{(2L)}^2} = \left(1 + \frac{\mu}{\sigma_n^2}\right) \frac{l(\mathbf{x})}{L} \mathcal{F}_{2l(\mathbf{x}),2L}, \quad (56)$$

where and $\mathcal{F}_{2l(\mathbf{x}),2L}$ denotes an F-distributed random variable with $2l(\mathbf{x})$ and $2L$ degrees of freedom. Now,

$$f(M(\mathbf{z})|\mathcal{H}_0) = f_{\mathcal{F}_{2l(\mathbf{x}),2L}} \left(\frac{M(\mathbf{z})L}{l(\mathbf{x})} \right) \quad (57)$$

$$f(M(\mathbf{z})|\mathcal{H}_1) = f_{\mathcal{F}_{2l(\mathbf{x}),2L}} \left(\frac{M(\mathbf{z})L}{l(\mathbf{x})(1 + \text{SNR})} \right). \quad (58)$$

where $f_{\mathcal{F}_{2l(\mathbf{x}),2L}}(\cdot)$ is the pdf of an $\mathcal{F}_{2l(\mathbf{x}),2L}$ random variable.

Since the pdf of the F distribution is monotonically decreasing, $f(M(\mathbf{z})|\mathcal{H}_1, \text{SNR})/f(M(\mathbf{z})|\mathcal{H}_0)$ is monotonically increasing. Consequently, (54) is equivalent to the following detector

$$T = M(\mathbf{z}) \underset{\mathcal{H}_1}{\overset{\mathcal{H}_0}{>}} \delta. \quad (59)$$

Since both the optimal test statistic T and δ are independent of the unknown parameters, (59) is a uniformly most powerful scale invariant detector [24]. \square

C. Discussion

Theorem 2 describes the optimal detector for the general detection problem in (50). In this subsection, we discuss this general problem in the context of the phased array, MIMO, and MISO radar systems. We compare the various systems based on their optimal scale invariant detector's SNR.

Denote by $\rho = E/\sigma_n^2$ the average received SNR. By using the same method leading to (43), (44), and (45), respectively, we have

$$\beta_{MIMO-UMPI} = \beta_{MIMO} \frac{(2L - 4)}{(2MN + 2L - 2)} \quad (60)$$

$$\beta_{\text{phased array-UMPI}} = \beta_{\text{phased array}} \frac{2L - 4}{2L} \quad (61)$$

$$\beta_{MISO-UMPI} = \beta_{MISO} \frac{2L - 4}{2L + 2M - 2} \quad (62)$$

From the expressions it is evident that the number of noise samples has great influence on the UMPI detectors' SNR. In each case, the SNR is equal to the optimal detector's SNR multiplied by a system dependent factor smaller than one. This factor represents the degradation in performance due to the unknown parameters, and it approaches one as the number of noise samples approaches infinity. This should not come as a surprise because, when the number of noise samples is high, the noise level can be estimated with very small error.

The number of independent noise samples we can obtain depends on the number of transmitters and receivers, the system complexity, and the model used. In clutter limited systems the only way to obtain samples of the noise process is to sample the output of the filters which are matched to the transmitted signals at locations (delays) that do not contain targets. In a typical radar system, between 8 and 16 such locations are used for estimating the noise level. Consider one such location [17]. In our proposed MIMO radar system, we can sample each of the MN matched filters at that delay and obtain MN independent samples of the noise process. Similar reasoning applies for the MISO system as well. In the phased array system, at each such location only N independent samples can be obtained because only one signal is transmitted by the transmitting array. Therefore, in practical radar systems we can expect about $10MN$ independent samples of the noise process if MIMO or MISO systems are used, and about $10N$ samples if a phased array radar systems are used.

Figures 4 and 5 depict the performance of the phased array, MIMO, and MISO radar systems' UMPI detectors. We consider two scenarios, in the first $M = 1$ and $N = 4$, while in the second $M = N = 4$. In addition, the number of independent samples of the noise process was set to either $8MN$ or MN . Figures 4 and 5 demonstrate the validity of our theoretical results. We can see that when the number of noise samples is large, the degradation in SNR is negligible. However, if the number of noise samples is very small, the degradation in the SNR of the MIMO and MISO systems is larger than that of the phased array system.

V. NUMERICAL EXAMPLES

In this section we consider several numerical examples which compare the performance of the various systems. These examples also validate the analysis conducted in the previous sections. In our first example we consider systems having 4 receiving antennas and 1 transmitting antenna, that is $N = 4$, $M = 1$. In this example, we consider both the MIMO radar system and the phased array radar system. Note that for $M = 1$, the MISO radar system is equivalent to the phased array radar system. Figure 6 depicts the probability of miss of the optimal detectors for known and unknown noise level, as a function of the SNR. The probability of false alarm was fixed at $P_{FA} = 10^{-6}$. The figure contains graphs for both known and unknown noise levels. In the case of unknown noise level, $L = 4$ and $L = 32$ independent samples of the noise process are used by the processor.

We can see that the results validate our analysis. At low SNR (for which the probability of detection is less than 0.5) the phased array system outperforms the MIMO system, while at high SNR the MIMO system outperforms the phased array system. Moreover, when the number of independent samples of the noise process is small, both the MIMO system and the phased array system exhibit large performance degradation, and the performance degradation of the MIMO system is much larger than the performance degradation of the phased array system. However, even for a moderate number of samples of the noise process, e.g., 32 samples, the performance degradation due to the unknown noise level is only about 1.5

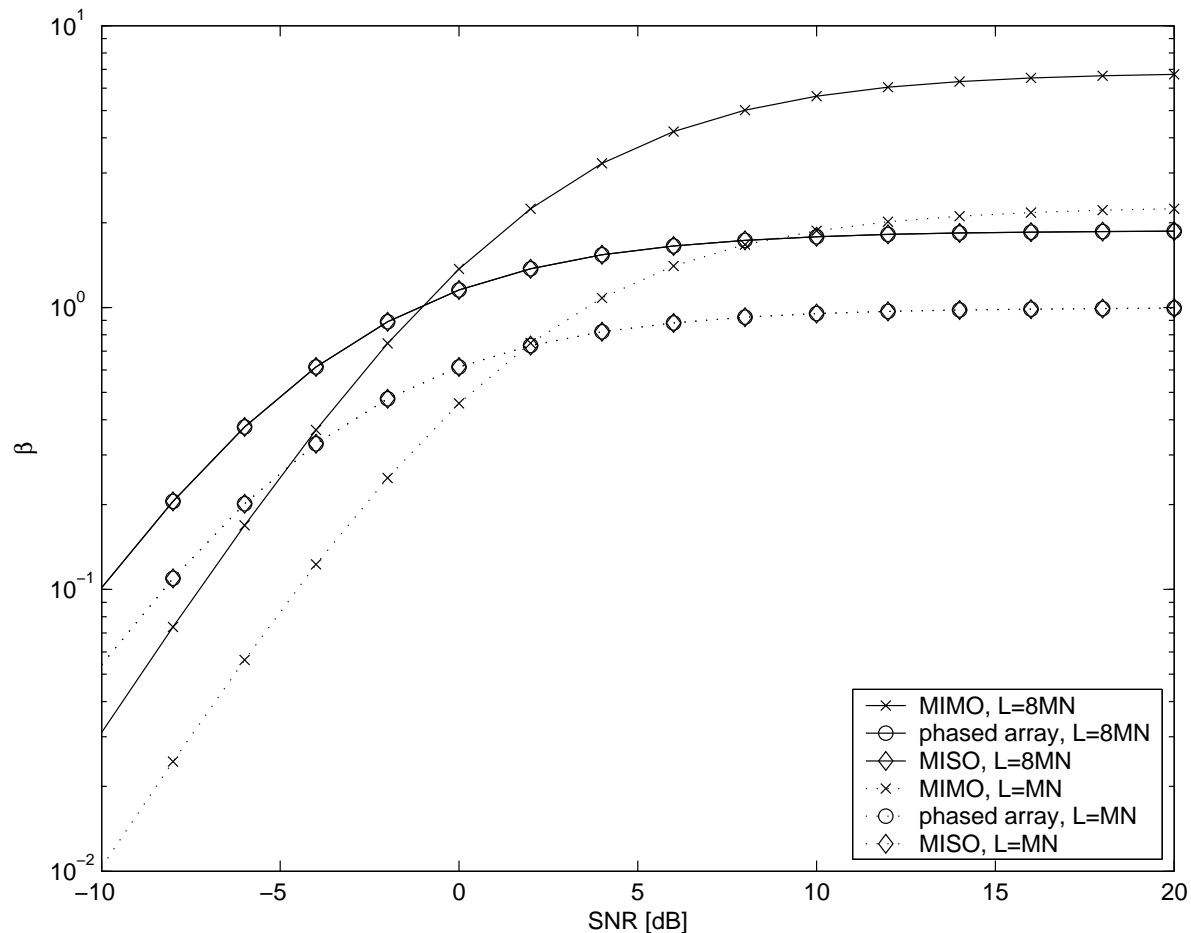


Fig. 4. The optimal detector's SNR for various systems. $M = 1$, $N = 4$.

dB.

Figure 7 depicts the receiver operating curves of the MIMO and phased array radar systems under known/unknown noise level conditions. The average received SNR was set at $\rho = 10$ dB. These results establish the advantage of the MIMO radar system over the phased array radar system. For known noise level, the MIMO radar system outperforms the phased array radar system even for very low probabilities of false alarm. For unknown noise level and 32 independent samples of the noise process, a MIMO radar system outperforms the phased array radar system whenever the probability of false alarm is greater than 10^{-8} .

In our second example we consider systems having 4 receiving antennas and 2 transmitting antennas, that is $N = 4$, $M = 2$. In this example, we consider the MIMO, MISO, and phased array systems. Figure 8 depicts the probability of miss of the optimal detectors for both known and unknown noise levels as a function of the SNR. The probability of false alarm was fixed at $P_{FA} = 10^{-6}$. We assume that when the

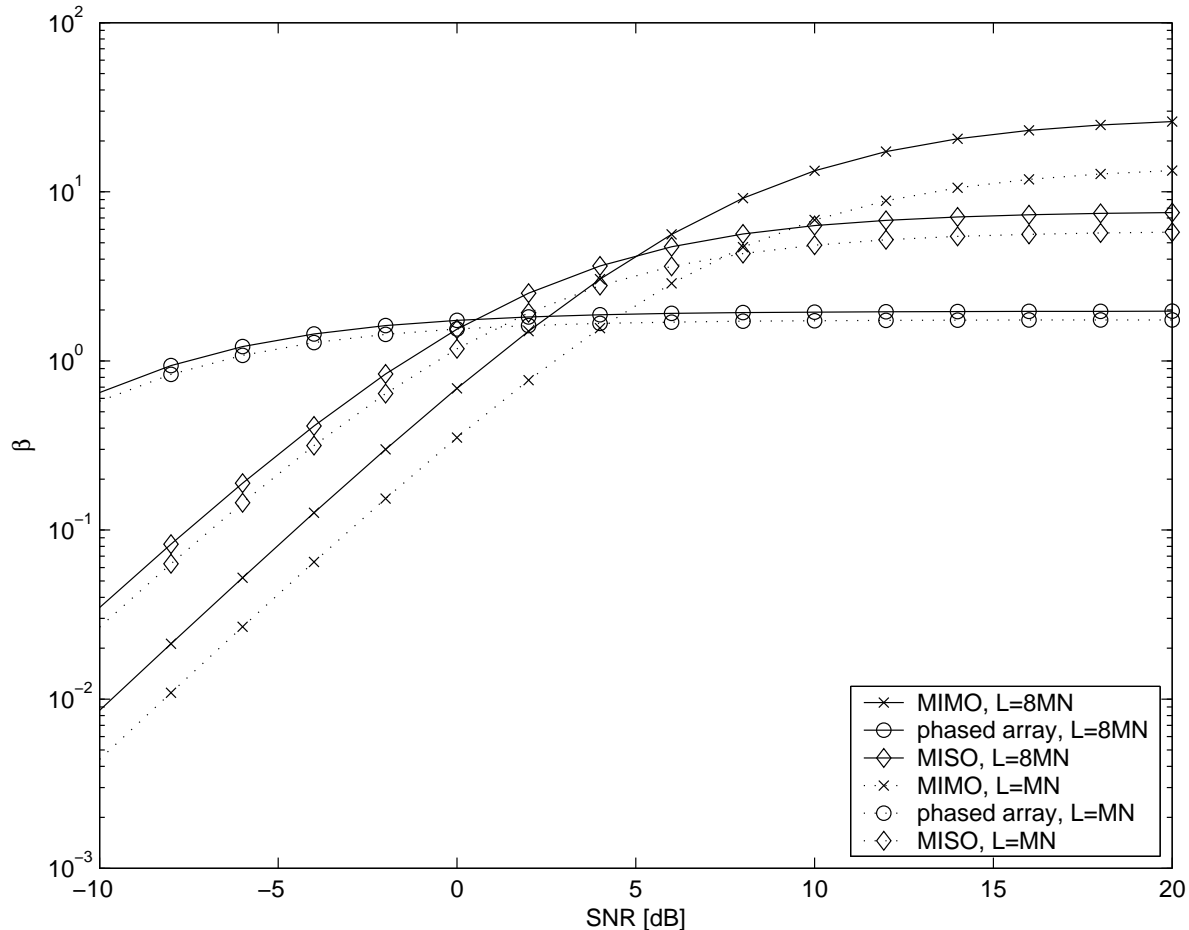


Fig. 5. The optimal detector's SNR for various systems. $M = N = 4$.

noise level is unknown the receiver obtains 64 independent samples of the noise process.

At low SNR the phased array system outperforms the MIMO system, while at high SNR the MIMO system outperforms the phased array system. However, we can see that the MIMO radar system outperforms the phased array system when the probability of miss is about 20%. We can also see from the results that the MISO system is, in a sense, a compromise between the MIMO and phased array systems. Therefore, at low SNR, the MISO system outperforms the MIMO system, while at high SNR the MISO system outperforms the phased array system.

Figure 9 depicts the receiver operating curves of the MIMO, MISO, and phased array radar systems under known noise level and unknown noise level conditions. The average received SNR was set at $\rho = 10$ dB. This figure establishes the advantage of the MIMO radar system over the phased array radar system. For known noise level, the MIMO system outperforms the phased array system at probability of false alarm greater than 10^{-8} ; whereas, for unknown noise level, the MIMO system outperforms the

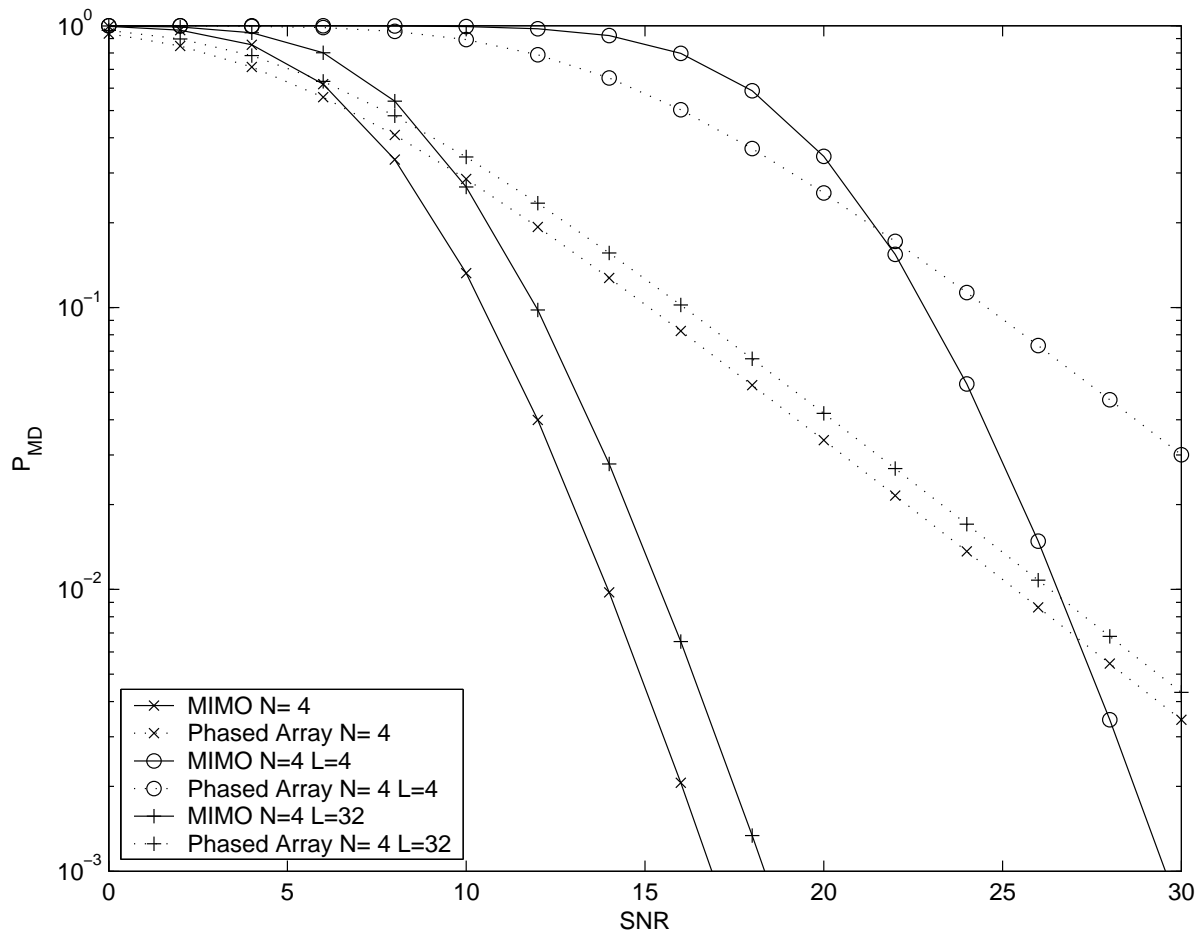


Fig. 6. Probability of detection as the function of the SNR, $N = 4, M = 1$. Note that the curves corresponding to the MISO and phased array radars fall on top of each other.

phased array system at a probability of false alarm greater than 10^{-6} . Again, the MISO system offers a compromise between the two systems.

VI. SUMMARY AND CONCLUDING REMARKS

In this paper, we introduced the concept of MIMO radar. This concept differs substantially from current regimes in which closely spaced antenna arrays are used. With closely spaced antenna elements it is possible to cohere a beam towards a direction in space and to realize a coherent processing gain. However, these systems are prone to severe target fading, and hence they may suffer considerable performance degradation. In contrast, MIMO radar can not cohere a beam toward a certain direction in space, and hence it can not realize any processing gain. However, MIMO radar exploits that target angular spread to combat target fading. MIMO radar is composed of many independent radars, each of which sees a different aspect of the target, enabling the MIMO radar to exploit spatial diversity to overcome target fading.

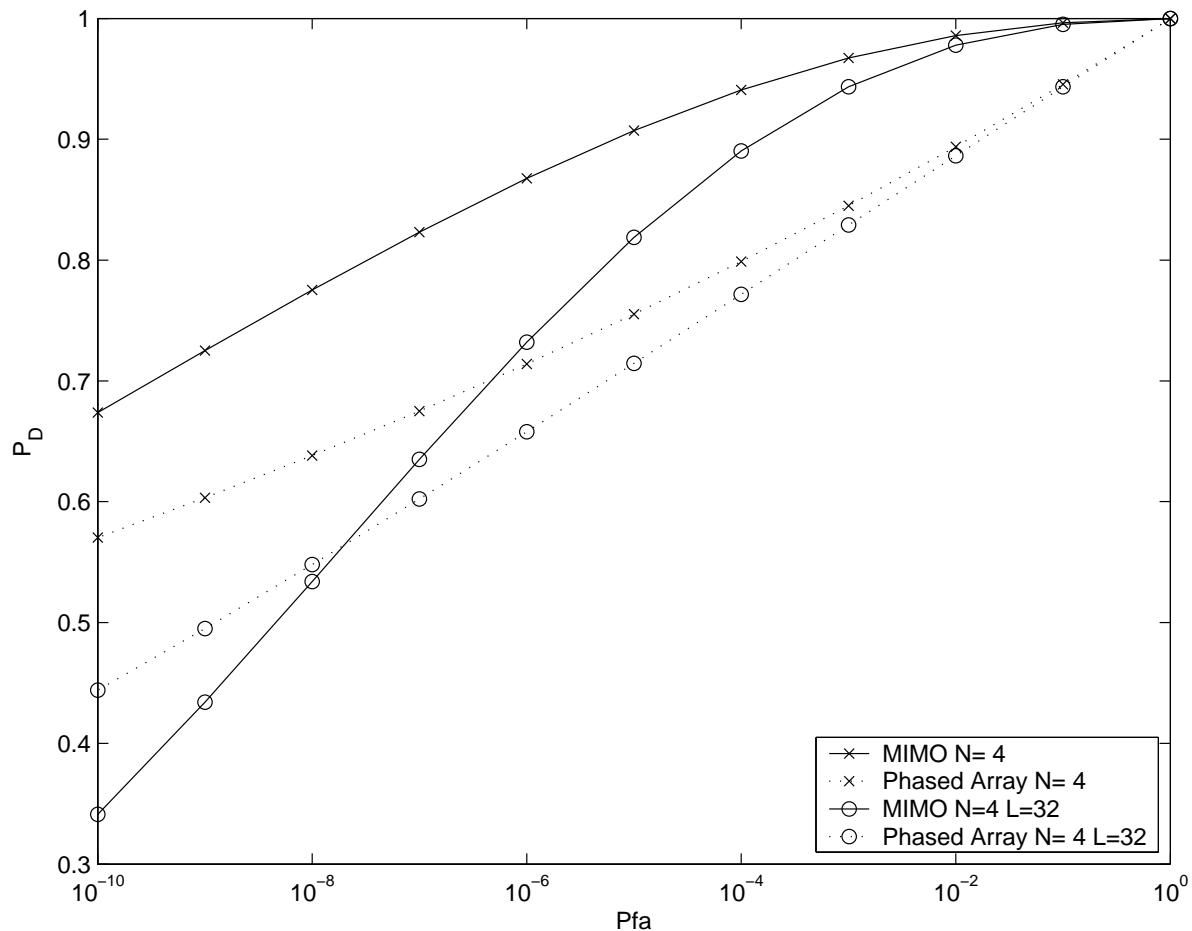


Fig. 7. Receiver's operating curves, $N = 4$, $M = 1$.

In addition, we extended the current models used in radar theory to account for both range and angular spreads, and sparse antenna arrays. While, for closely spaced arrays, this model is equivalent to the current existing models, for sparse antenna arrays, this model provides for the first time a simple method for modeling the signals received from complex targets. In addition, this model offers insights into the advantages and disadvantages of each system considered in this paper. From the model we can learn how MIMO radar can exchange coherent processing gain for diversity gain.

More importantly, we investigated and compared the inherent performance limitations of both conventional phased array radars and the newly proposed radars. We derived the optimal detectors for both the conventional and the newly proposed systems when the parameters are either known or unknown. We demonstrated that the MIMO radar outperforms the conventional phased array radar whenever the probability of detection is at a reasonable level, say above 80%.

So far, we have ignored the fact that, in practice, a phased array radar system needs to scan the whole

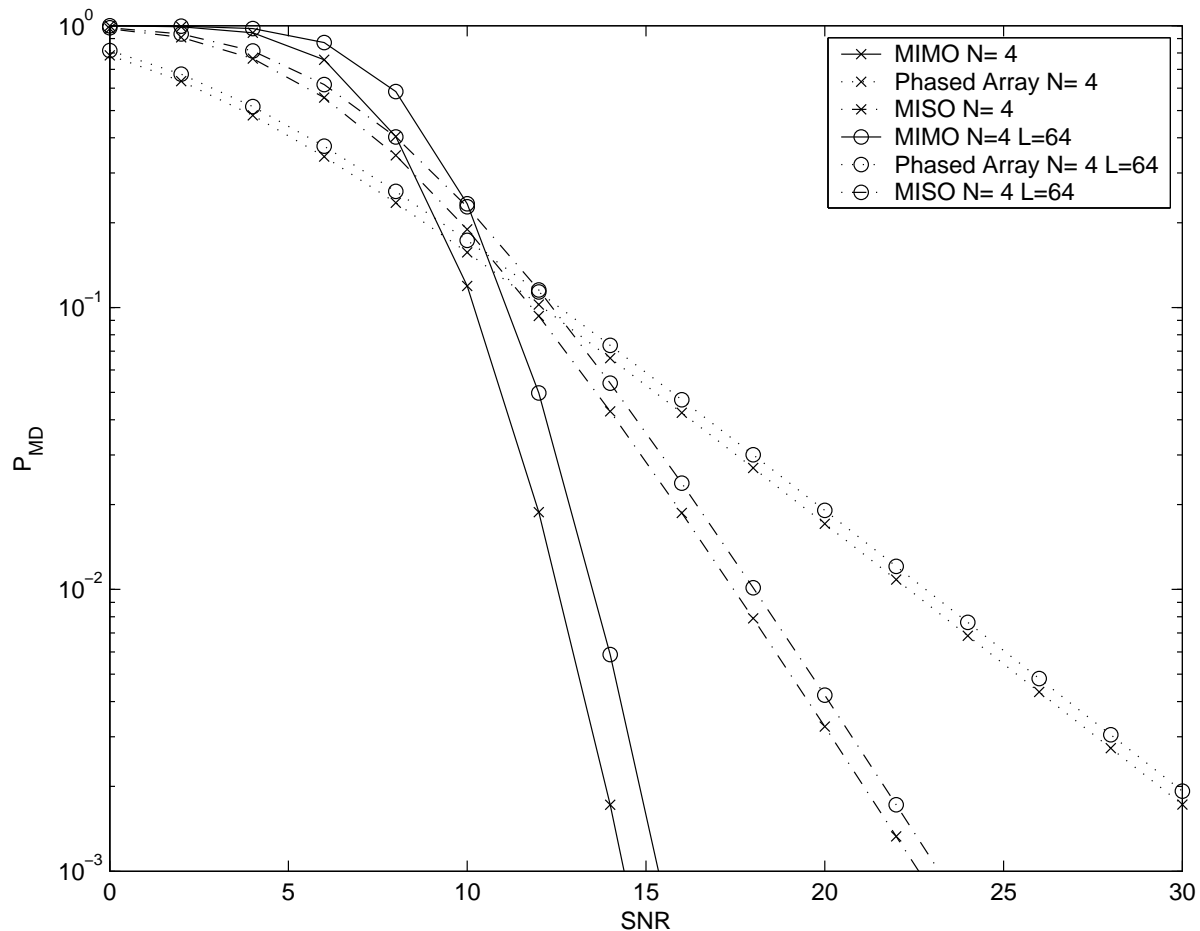


Fig. 8. Probability of detection as a function of the SNR, $N = 4$, $M = 2$.

space. Once a phased array radar system realizes a processing gain of M , it needs M times more time to scan the whole space. If we compare the MIMO system and the phased array system under the constraint that both systems need to scan the whole space and use the same total energy for accomplishing this task, phased array radar systems incur an SNR loss of $10\log_{10}M$ dB compared with the SNR of the MIMO systems. Therefore, in practical systems, the advantage of MIMO system is even greater than the one reported here.

It is the current state of understanding that one should always try to increase the SNR by coherent combining. In this paper, we suggest to deviate from this regime and to balance between coherent processing and diversity. This paper provides a partial answer to the problem we refer to as “detection with unit energy.” This problem is defined as follows: given a fixed amount of energy and a scintillating target, should we cohere a beam toward the target and see only one aspect of the target or observe several aspects of the target with reduced power. Another aspect of the same problem is the need to decide

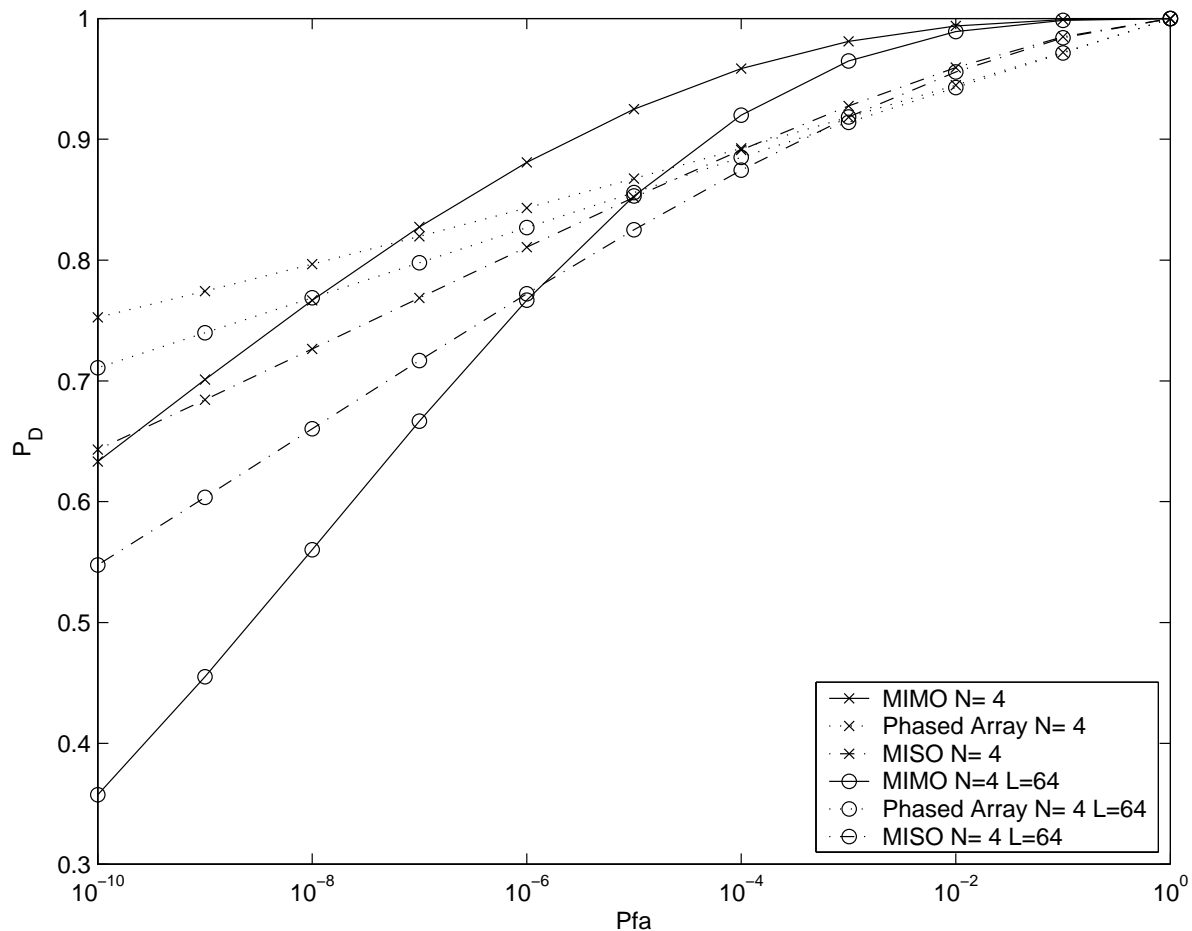


Fig. 9. Receiver's operating curves, $N = 4$, $M = 2$.

whether to transmit one strong pulse or to divide our energy between several pulses?

The performance improvement achieved by MIMO radar is not limited to detection. In subsequent papers, we will provide a detailed analysis which demonstrates the superiority of MIMO radar in many aspects over the conventional phased array radar. We show that MIMO radar enjoys lower range, location, angle of arrival, and Doppler estimation errors. A preliminary analysis that demonstrates these results can be found in [22], [31].

REFERENCES

- [1] W. M. Siebert, "A radar detection philosophy," *IEEE Trans. on Information Theory*, vol. 2, pp. 204–221, Sep. 1956.
- [2] M. Skolnik, *Introduction to Radar Systems*. McGraw-Hill, 3rd ed., 2002.
- [3] P. M. Woodward, *Probability and Information Theory with Application to Radar*. Artech House Books, MA, 1953.
- [4] H. L. V. Trees, *Detection, Estimation, and Modulation Theory*, vol. III. John Wiley & Sons, NY, 1968.
- [5] S. Haykin, J. Litva, and T. J. Shepherd, *Radar Array Processing*. New York: Springer - Verlag, 1st ed., 1993.

- [6] A. Dogandzic and A. Nehorai, "Cramer-Rao bounds for estimating range, velocity, and direction with an active array," *IEEE Trans. on Signal Processing*, vol. 49, pp. 1122–1137, June 2001.
- [7] S. Pasupathy and A. N. Venetsanopoulos, "Optimum active array processing structure and space-time factorability," *IEEE Trans. Aerospace and Electronic Systems*, vol. 10, pp. 770–778, 1974.
- [8] L. Swindlehurst and P. Stoica, "Maximum likelihood methods in radar array signal processing," *Proc. of the IEEE*, vol. 86, pp. 421–441, Feb. 1998.
- [9] A. Farina, *Antenna Based Signal Processing Techniques for Radar Systems*. Norwood, MA: Artech House, 1992.
- [10] H. Wang and L. Cai, "On adaptive spatio-temporal processing for airborne surveillance radar systems," *IEEE Trans. on Aerospace and Electronic Systems*, vol. 30, pp. 660–669, July 1994.
- [11] J. Ward, "Cramer-Rao bounds for target angle and Doppler estimation with space-time adaptive processing radar," in *Proc. 29th Asilomar Conf. Signals, Syst. Comput.*, pp. 1198–1202, Nov. 1995.
- [12] C. Baixiao, Z. Shouhong, W. Yajun, and W. Jun, "Analysis and experimental results on sparse array synthetic impulse and aperture radar," in *Proc. 2001 CIE International Conference on Radar*, pp. 76–80, Oct. 2001.
- [13] C. Baixiao, L. Hongliang, and Z. Shouhong, "Long-time coherent integration based on sparse-array synthetic impulse and aperture radar," in *Proc. 2001 CIE International Conference on Radar*, pp. 76–80, Oct. 2001.
- [14] J. M. Colin, "Phased array radars in France: Present and future," in *Proc. IEEE Int. Symp. on Phased Array Systems and Technology*, pp. 458–462, Oct. 1996.
- [15] A. S. Fletcher and F. C. Robey, "Performance bounds for adaptive coherence of sparse array radar," in *Proc. of the 11th conf. on Adaptive Sensors Array Processing*, Mar. 2003.
- [16] D. Rabideau, "Ubiquitous MIMO digital array radar," in *Proc. of the Asilomar Conference on Signals, Systems, and Computers*, November 2003.
- [17] N. Levanon, *Radar Principles*. John Wiley & Sons, 1st ed., 1988.
- [18] G. J. Foschini, "Layered space-time architecture for wireless communication in a fading environment when using multiple antennas," *Bell Labs Technical Journal*, vol. 1, no. 2, pp. 41–59, 1996.
- [19] F. Friedmann, R. Raich, J. Goldberg, and H. Messer, "Bearing estimation for a distributed source of nonconstant modulus bounds and analysis," *IEEE Trans. on Signal Processing*, vol. 51, pp. 3027–3035, Dec. 2003.
- [20] Y. U. Lee, J. Choi, I. Song, and S. R. Lee, "Distributed source modeling and direction-of-arrival estimation techniques," *IEEE Trans. on Signal Processing*, vol. 45, pp. 960–969, Apr. 1997.
- [21] R. Raich, J. Goldberg, and H. Messer, "Bearing estimation for a distributed source: Modeling, inherent accuracy limitations and algorithms," *IEEE Trans. on Signal Processing*, vol. 48, pp. 429–441, Feb. 2000.
- [22] E. Fishler, A. Haimovich, R. Blum, L. Cimini, D. Chizhik, and R. Valenzuela, "MIMO radar: An idea whose time has come," in *Proc. of the IEEE Int. Conf. on Radar*, April Philadelphia, PA, 2004.
- [23] H. L. V. Trees, *Detection, Estimation, and Modulation Theory*, vol. I. John Wiley & Sons, NY, 1968.
- [24] E. L. Lehmann, *Testing Statistical Hypotheses*. John Wiley & Sons, 2nd ed., 1986.
- [25] J. B. Lewis and P. M. Schultheiss, "Optimum and conventional detection using a linear array," *The Journal of the Acoustical Society of America*, vol. 49, pp. 1083–1091, Apr. 1971.
- [26] L. L. Scharf, *Statistical Signal Processing: Detection, Estimation, and Time Series Analysis*, vol. 2nd. Pearson Education, 2002.
- [27] P. Grieve, "The optimum constant false alarm probability detector for relatively coherent multichannel signals in gaussian noise of unknown power," *IEEE Trans. on Information Theory*, vol. 23, pp. 708–721, Nov. 1977.
- [28] L. Scharf and D. Lytle, "Signal detection in gaussian noise of unknown level: An invariance application," *IEEE Trans. on Inf. Theory*, vol. 17, pp. 404–411, July 1971.
- [29] T. S. Ferguson, *Mathematical Statistics: A decision Theoretic Approach*. Probability and Mathematical Statistics, Academic Press, NY, 1967.
- [30] S. Kay, *Fundamentals of Statistical Signal Processing: Part II*. Prentice Hall, 1998.
- [31] E. Fishler, A. Haimovich, R. Blum, L. Cimini, D. Chizhik, and R. Valenzuela, "Statistical MIMO radar," in *The 12th conf. on Adaptive Sensors Array Processing*, March 2004.

APPENDICES

I. PROOF OF LEMMA 1

In this section we compute the LRT detector for MIMO radar systems. We start by deriving the pdf of the received measurements under both the null and alternative hypotheses. Consider first the alternative hypothesis.

$$\begin{aligned}
f(\mathbf{r}(t)|\mathcal{H}_1) &= \int f(\mathbf{r}(t)|\mathcal{H}_1, \boldsymbol{\alpha}) f(\boldsymbol{\alpha}) d\boldsymbol{\alpha} = \int c e^{-\frac{1}{\sigma_n^2} \int \|\mathbf{r}(t) - \mathbf{H} \sqrt{\frac{E}{M}} \mathbf{s}(t-\tau)\|^2 dt} f(\boldsymbol{\alpha}) d\boldsymbol{\alpha} \\
&= \int c e^{-\frac{1}{\sigma_n^2} \sum_i \int |r_i(t) - \sqrt{\frac{E}{M}} \sum_{j=1}^M \alpha_{ij} s_j(t-\tau)|^2 dt} f(\boldsymbol{\alpha}) d\boldsymbol{\alpha} \\
&\stackrel{(a)}{=} \int c e^{-\frac{1}{\sigma_n^2} \sum_i \int |r_i(t)|^2 dt - \sqrt{\frac{E}{M}} \sum_{j=1}^M \alpha_{ij}^* \int r(t) s_j^*(t-\tau) dt - \sqrt{\frac{E}{M}} \sum_{j=1}^M \alpha_{ij} \int r^*(t) s_j(t-\tau) dt + \frac{E}{M} \sum_{j=1}^M |\alpha_{ij}|^2} f(\boldsymbol{\alpha}) d\boldsymbol{\alpha} \\
&= c' e^{-\frac{\int \|\mathbf{r}(t)\|^2 dt}{\sigma_n^2}} \int e^{-\frac{1}{\sigma_n^2} (-\sqrt{\frac{E}{M}} \boldsymbol{\alpha}^H \mathbf{x} - \sqrt{\frac{E}{M}} \mathbf{x}^H \boldsymbol{\alpha} + \|\sqrt{\frac{E}{M}} \boldsymbol{\alpha}\|^2)} e^{-\|\boldsymbol{\alpha}\|^2} d\boldsymbol{\alpha} \\
&= c' e^{-\frac{\int \|\mathbf{r}(t)\|^2 dt}{\sigma_n^2} + \frac{\frac{E}{M} \|\mathbf{x}\|^2}{\sigma_n^2 (\sigma_n^2 + \frac{E}{M})}} \int e^{-\frac{1}{\sigma_n^2} \left\| \sqrt{\sigma_n^2 + \frac{E}{M}} \boldsymbol{\alpha} - \frac{\sqrt{\frac{E}{M}} \mathbf{x}}{\sqrt{\sigma_n^2 + \frac{E}{M}}} \right\|^2} d\boldsymbol{\alpha} = c'' e^{-\frac{\int \|\mathbf{r}(t)\|^2 dt}{\sigma_n^2} + \frac{\frac{E}{M} \|\mathbf{x}\|^2}{\sigma_n^2 (\sigma_n^2 + \frac{E}{M})}} \quad (63)
\end{aligned}$$

where \mathbf{x} is an $NM \times 1$ vector such that $[\mathbf{x}]_{iN+j} \triangleq \int r_i(t) s_j(t-\tau) dt$, $\boldsymbol{\alpha}$ is the $NM \times 1$ vector that contains the fading coefficients, and in (a) we use the fact that $\int s_j(t) s_i(t) dt = \delta_{ij}$.

The pdf of the received measurements under the null hypothesis is given by,

$$f(\mathbf{r}(t)|\mathbf{H}_0) = c e^{-\frac{\int \|\mathbf{r}(t)\|^2 dt}{\sigma_n^2}} \quad (64)$$

Combining (63), (64), and (23) results in the following detector,

$$T = \log f(\mathbf{r}(t)|\mathbf{H}_1) - \log f(\mathbf{r}(t)|\mathcal{H}_0) = \|\mathbf{x}\|^2 \underset{\mathbf{H}_0}{<} \underset{\mathbf{H}_1}{>} \delta. \quad (65)$$

II. PROOF OF LEMMA 2

In order to prove Lemma 2, we need to derive the pdf of the received measurements under both the null and alternative hypotheses. We first consider the alternative hypothesis.

$$\begin{aligned}
f(\mathbf{r}(t)|\mathcal{H}_1) &= \int f(\mathbf{r}(t)|\mathcal{H}_1, \boldsymbol{\alpha}) f(\boldsymbol{\alpha}) d\boldsymbol{\alpha} = \int c e^{-\frac{1}{\sigma_n^2} \int \|\mathbf{r}(t) - \sqrt{\frac{E}{M}} \boldsymbol{\alpha} \mathbf{a}(\theta) \mathbf{b}^H(\theta') \bar{\mathbf{b}} s(t-\tau)\|^2 dt} f(\boldsymbol{\alpha}) d\boldsymbol{\alpha} \\
&= c e^{-\frac{\int \|\mathbf{r}(t)\|^2 dt}{\sigma_n^2}} \int e^{-\frac{1}{\sigma_n^2} (-2\sqrt{\frac{E}{M}} \Re(\boldsymbol{\alpha} \mathbf{b}^H(\theta') \bar{\mathbf{b}} \int \mathbf{r}^H(t) \mathbf{a}(\theta) s(t-\tau) dt) + \frac{E}{M} |\boldsymbol{\alpha}|^2 \|\bar{\mathbf{b}}^H \mathbf{b}(\theta) \mathbf{a}(\theta)\|^2) + |\boldsymbol{\alpha}|^2} d\boldsymbol{\alpha} \\
&= c' e^{-\frac{\int \|\mathbf{r}(t)\|^2 dt}{\sigma_n^2} - \frac{E |\mathbf{b}(\theta') \bar{\mathbf{b}}|^2 \|\int \mathbf{r}^H(t) \mathbf{a}(\theta) s(t-\tau) dt\|^2}{M \sigma_n^2 (1 + \frac{E}{M} |\mathbf{b}(\theta') \bar{\mathbf{b}}|^2)}} = c' e^{-\frac{\int \|\mathbf{r}(t)\|^2 dt}{\sigma_n^2} - \frac{E |\mathbf{b}(\theta') \bar{\mathbf{b}}|^2 |x|^2}{M \sigma_n^2 (1 + \frac{E}{M} |\mathbf{b}(\theta') \bar{\mathbf{b}}|^2)}}, \quad (66)
\end{aligned}$$

where $x = \int \mathbf{r}^H(t) \mathbf{a}(\theta) s(t-\tau) dt$.

The pdf of the received measurements under the null hypothesis is given by (64). Combining (66), (64), and (23) results in the following detector,

$$T = \log f(\mathbf{r}(t)|\mathbf{H}_1) - \log f(\mathbf{r}(t)|\mathcal{H}_0) = \int \mathbf{r}^H(t) \mathbf{a}(\theta) s(t-\tau) dt \underset{\mathbf{H}_0}{>} \underset{\mathbf{H}_1}{<} \delta. \quad (67)$$